CHAPTER IV
RESULTS AND DISCUSSION

Effects of adsorbate concentration, zeolite type and temperature were studied here. *KBaX* and *KY* zeolites were chosen as the adsorbents for this study. Roughly, concentrations of each C_8 aromatics were varied from 1.25 to 20% by weight at the temperatures of 40, 65 and 90°C. All experiment data are given in Appendix.

Effect of adsorbate concentration

Figure 4.1 shows the adsorptions of *p*-xylene, *m*-xylene, *o*-xylene and ethylbenzene on the *KBaX* zeolite at 40°C. The amount of a C_8 aromatic adsorbed is expressed in gram of the adsorbed species per gram of zeolite, and this is also called loading. According to Figure 4.1, at high xylene/toluene mole ratios, the zeolite adsorbs *p*-xylene more than the other aromatics. On one hand, *o*-xylene is the least adsorbed species by the zeolite at high xylene/toluene mole ratios. On the other hand, at low xylene/toluene mole ratios, *o*-xylene is the most adsorbed aromatics. It can not explain because mechanism don't understand in this moment.

The same result was also observed at 65°C as shown in Figure 4.2. However, at 65°C, the amount of each aromatic adsorbed by the *KBaX* zeolite is about 30% less than that at 40°C. *O*-xylene is also adsorbed more than the other species at low xylene/toluene mole ratios but in a lesser extent. This can be explained by the known fact that the adsorption process is exothermic. Therefore, the zeolite adsorbs all the species less at higher temperatures.

Figure 4.3 shows the adsorption of the C_8 aromatics adsorbed by the *KBaX* zeolite at 90°C. A few differences in the adsorption at this temperature compared to the other two temperatures can be observed. First, at low

xylene/toluene mole ratios, the zeolite adsorbs about the same trend for every species. Next is the zeolite adsorbs about the same amount of *m*-xylene and ethylbenzene at high xylene/toluene mole ratios. Again, the adsorption of every species by the zeolite is less than what has been observed at the other temperatures.

Figure 4.4 shows the adsorptions of *p*-xylene, *m*-xylene, *o*-xylene and ethylbenzene on the *KY* zeolite at 40°C. According to the figure, at high xylene/toluene mole ratios, the zeolite adsorbs *p*-xylene more than the other aromatics. But at low xylene/toluene mole ratios, the amounts of the C_8 aromatics adsorbed are nearly the same. The behavior that the *KBaX* zeolite adsorbs more *o*-xylene than the other species at low xylene/toluene mole ratios can not be noticed with the *KY* zeolite. A simple explanation could be that the size of the α-cage of the *KY* zeolite is bigger than that of the *KBaX* zeolite. Hence, the effect of the aromatic's structure plays little role in the adsorption at low xylene/toluene mole ratios. This reason can be further supported by the results form the Brunaner Emmett Teller (BET) analysis as shown in Table 3.5. The BET results show that the micropore volume, surface area and average pore diameter of the *KY* zeolite are greater than those of the *KBaX* zeolite.

The same result is also observed at 65 and 90°C as shown in Figures 4.5 and 4.6. However, at 65 and 90°C, the amounts of each aromatic adsorbed by the *KY* zeolite is about 20% and 30% less than that at 40°C, respectively. Like the results at 40°C, the amounts of the C_8 aromatics adsorbed are nearly the same at low xylene/toluene mole ratios.

Effect of zeolite type

Comparison of *p*-xylene and toluene adsorptions on the *KBaX* and *KY* zeolites at 40°C is shown in Figure 4.7. at low xylene/toluene mole ratios, the amounts of both *p*-xylene and toluene adsorbed on each zeolite are comparable. But at high xylene/toluene mole ratios, both zeolites adsorb more *p*-xylene

compared to toluene. Figure 4.7 also further emphasizes that the *KY* zeolite adsorbs more *p*-xylene and toluene than the *KBaX* zeolite does. Adsorptions of *p*-xylene and toluene on the zeolites at 65 and 90°C are shown in Figures 4.8 and 4.9. The adsorption at both temperatures exhibits the same trend as what has been observed at 40°C.

Adsorptions of *m*-xylene/toluene and *o*-xylene/toluene on the *KBaX* and *KY* zeolites at 40, 65 and 90°C are plotted in Figures 4.9–4.14. The *KY* zeolite adsorbs more toluene than *m*-xylene and *o*-xylene over the range of the temperature. One important point that should be made here is the amount of toluene adsorbed relative to *m*-xylene or *o*-xylene by the *KY* zeolite is much higher than that in the case of the *KBaX* zeolite. The point holds true for the three temperatures.

The *KBaX* and *KY* zeolites adsorb ethylbenzene and toluene the same way they do with m-xylene/toluene and o-xylene/toluene. The results at 40, 65 and 90°C are shown in Figures 4.15, 4.16 and 4.17, respectively. The main difference, however, is the *KBaX* zeolite adsorbs about the same amount of ethylbenzene and toluene. This may be explained by the effects of typeof the zeolite. Because zeolite *X* has higher exchange capacity for cation in site. It may be increase adsorbate and adsorbent interaction. Therefore, the *KY* zeolite has an ability to absorb more C_8 aromatics than the *KBaX* zeolite does.

Effect of temperature

At the full capacity of both zeolites, selectivity of *p*-xylene relative to the other C_8 aromatics and toluene on the *KBaX* and *KY* zeolites as a function of temperature is shown in Figures 4.19 and 4.20. Both figures clearly indicate that temperature has very little effect on the selectivity for both zeolites on adsorbing *p*-xylene from toluene and the other C_8 aromatics over the range of the temperature. On the *KBaX* zeolite, *p*-xylene/*o*-xylene shows higher selectivity than *p*-xylene/*m*-xylene, *p*-xylene/toluene and *p*-xylene/ethylbenzene. In other

words, the *KBaX* zeolite adsorbs more *p*-xylene than the other aromatics. It is worth noting that the *KBaX* zeolite shows comparable selectivity of *p*-xylene/toluene and *p*-xylene/ethylbenzene. The same trend can be observed in the case of the *KY* zeolite. Except the adsorptions of *p*-xylene/toluene and *p*-xylene/ethylbenzene that possess about the same selectivity on both *KBaX* and *KY* zeolites, the selectivity of *p*-xylene/*o*-xylene and *p*-xylene/*m*-xylene is higher on the *KY* zeolite.

Figures 4.21 and 4.22 show selectivity at the full capacity of both zeolites of the C_8 aromatics relative to toluene on the *KBaX* and *KY* zeolites as a function of temperature. Both figures clearly indicate that temperature has very little effect on the selectivity for both zeolites on adsorbing *p*-xylene from toluene over the range of the temperature. On the *KBaX* zeolite, the selectivity of *p*-xylene/toluene is more than one meaning that the zeolite preferably adsorbs more *p*-xylene. The selectivity of ethylbenzene/toluene is close to one implying that ethylbenzene is not preferentially adsorbed compared to toluene by the *KBaX* zeolite. Moreover, the *KBaX* zeolite selectively adsorbs more toluene than *m*-xylene and *o*-xylene as shown by the selectivity of *m*-xylene/toluene and *o*-xylene/toluene is less than one. The same trend can be observed in the case of the *KY* zeolite. The *KY* zeolite selectively adsorbs *p*-xylene more than toluene while it adsorbs more toluene than the other C_8 aromatics. Because of both zeolites selectivity on *p*-xylene and toluene compared to *m*-xylene, *o*-xylene and ethylbenzene, they make excellent choices for *p*-xylene separation from mixtures of the C_8 aromatics.

Modeling

The simplest approach to correlate liquid phase equilibrium data is to represent the equilibrium in terms of a concentration-dependent distribution coefficient (Ching *et al.*, 1990). The model can be written as

$$K = \frac{q}{c} = k + AC^{m} \tag{4.1}$$

where q is solute concentration based on particle volume (g/cm^3) and c is solute concentration in bulk phase (g/cm^3). When the curvature of the equilibrium line is not too great, linear expression of equion 4.1 can be obtained by setting m equal to 1. Parameter k is the apparent Herry's law constant, the slope of the equilibrium line at infinite dilution. It follows immediately from equation 4.1 that A and m may easily be determined from the experimental data over a range concentrations by regression (Ching et al., 1990). In this work, m was equal to one, k and A were determined by fitting the equation to the experimental data from low xylene/toluene to the ratio where the zeolite reach its full capacity. The parameters are reported in Table 4.1.

The comparison of experiment data and model prediction of p-xylene, m-xylene, ethylbenzene and o-xylene on the KBaX zeolite in the p-xylene/toluene, m-xylene/toluene, ethylbenzene/toluene and o-xylene/toluene systems at 40, 65 and 90°Cis shown in Figures 4.23 to 4.26. According to the figures, the distribution coefficients at low temperature are higher than that at high temperature. This means that, before the zeolite reaches its full capacity, the zeolite adsorbs more C$_8$aromatics at low temperature. The slope shows the effect of concentration on the distribution coefficient. All slopes of the C$_8$ aromatics are positive except the slope of o-xylene is likely to be adsorbed more easily with its compact structure, and that results in the higher distribution coefficient at low o-xylene equilibrium concentration in the liquid phase. The constant k at low temperature is higher than that at high temperature.

The comparison of experiment data and model prediction of p-xylene, m-xylene, ethylbenzene and o-xylene on the KBaX zeolite in the p-xylene/toluene, m-xylene/toluene, ethylbenzene/toluene and o-xylene/toluene systems at 40, 65 and 90°C, Figures 4.27 to 4.30 shows. The same trend of the distributioncoefficients that they are higher at low temperature is observed for

the *KY* zeolite. All slopes of the C_8 aromatics at 65 and 90°C are positive except the slope of *m*-xylene, ethylbenzene and *o*-xylene at 40°C.

The comparison of experiment data and model prediction of toluene on the *KBaX* zeolite in the *p*-xylene/toluene, *m*-xylene/toluene, ethylbenzene/toluene and *o*-xylene/toluene systems at 40, 65 and 90°C is shown in Figures 4.31 to 4.38. According to the figures, the distribution coefficient at low temperature is more than that high temperature. All slopes are nearly zero. That simply implies that the distribution coefficient is not sensitive to the increasing of temperature.

Table 4.1 The parameters for the distribution coefficient equation.

	The *KBaX* zeolite					
	40°C		65°C		90°C	
	A	*k*	*A*	*k*	*A*	*k*
p-xylene	8.596	0.464	3.673	0.295	4.615	0.114
toluene with *p*-xylene	-0.320	0.277	-0.273	0.235	-0.211	0.182
m-xylene	0.787	0.423	3.341	0.226	0.463	0.175
toluene with *m*-xylene	-0.357	0.308	-0.327	0.281	-0.236	0.203
ethylbenzene	16.234	0.135	13.186	0.004	4.181	0.056
toluene with ethylbenzene	-0.380	0.327	-0.351	0.301	-0.264	0.226
o-xylene	-29.222	1.251	-10.767	0.597	-0.493	0.169
toluene with *o*-xylene	-0.300	0.262	-0.266	0.232	-0.252	0.217
	The *KY* zeolite					
	40°C		65°C		90°C	
	A	*k*	*A*	*k*	*A*	*k*
p-xylene	56.289	0.223	33.225	0*	24.584	0*
toluene with *p*-xylene	-0.512	0.440	-0.495	0.425	-0.425	0.365
m-xylene	-0.111	0.634	3.119	0.341	6.148	0.114
toluene with *m*-xylene	-0.552	0.472	-0.593	0.505	-0.520	0.443
ethylbenzene	-3.617	0.998	16.798	0.251	16.317	0*
toluene with ethylbenzene	-0.566	0.490	-0.540	0.465	-0.496	0.426
o-xylene	-8.670	0.728	0.668	0.315	4.494	0.120
toluene with *o*-xylene	-0.533	0.463	-0.502	0.434	-0.474	0.408

* could not be regressed with certainty. They were set to zero.
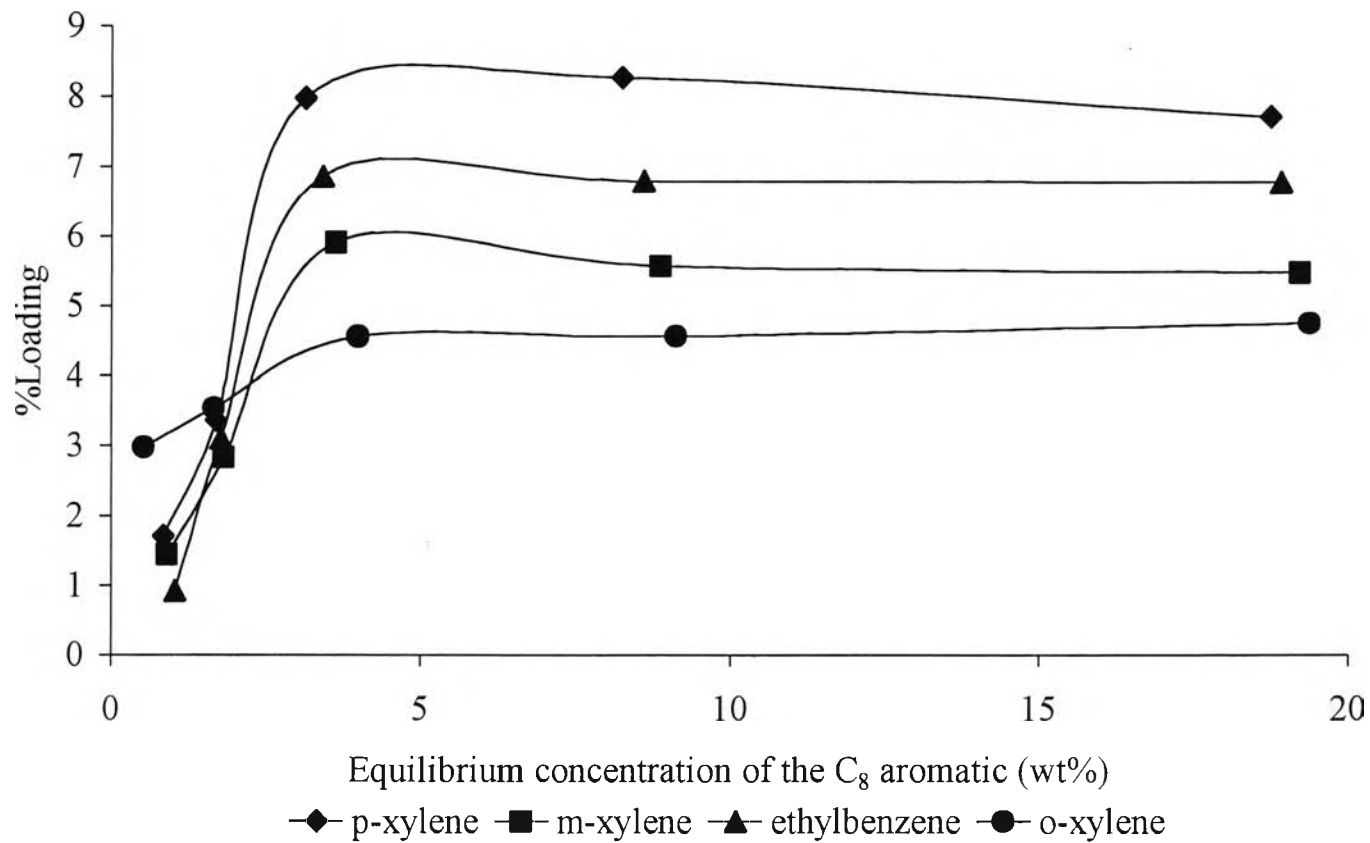
Figure 4.1 Adsorption of the C$_8$ aromatics on the *KBaX* zeolite at 40°C.
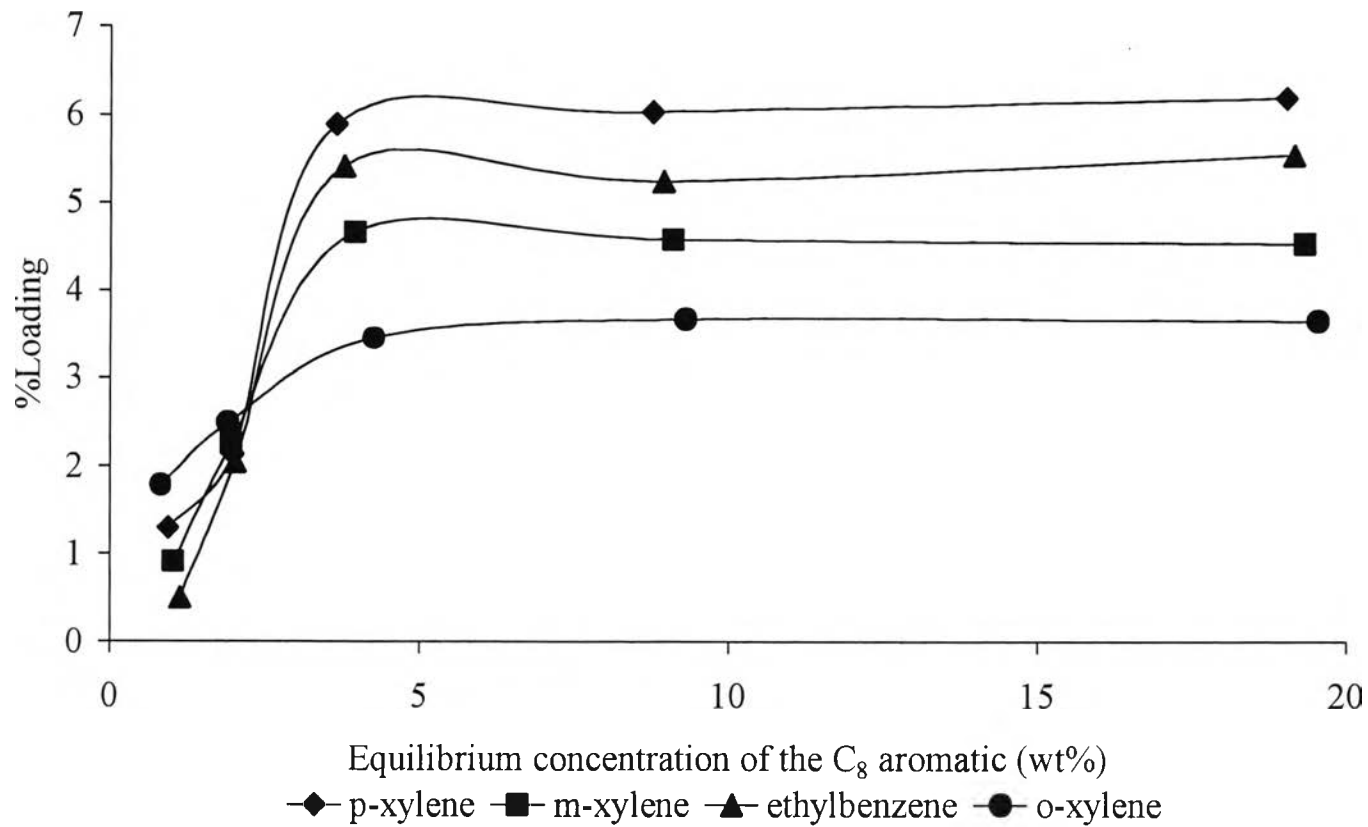
Figure 4.2 Adsorption of the C_8 aromatics on the *KBaX* zeolite at 65°C.
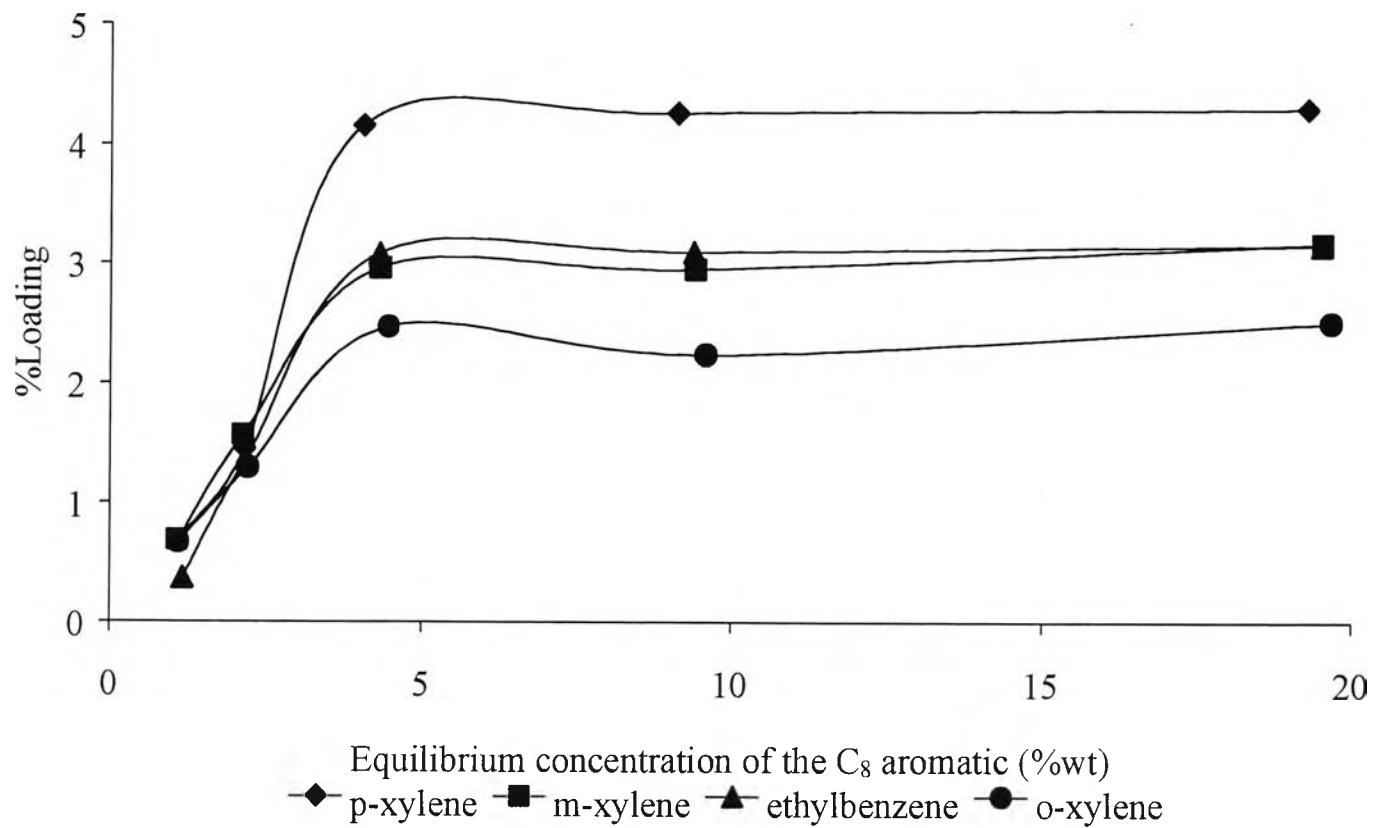
Figure 4.3 Adsorption of the C_8 aromatics on the *KBaX* zeolite at 90°C.
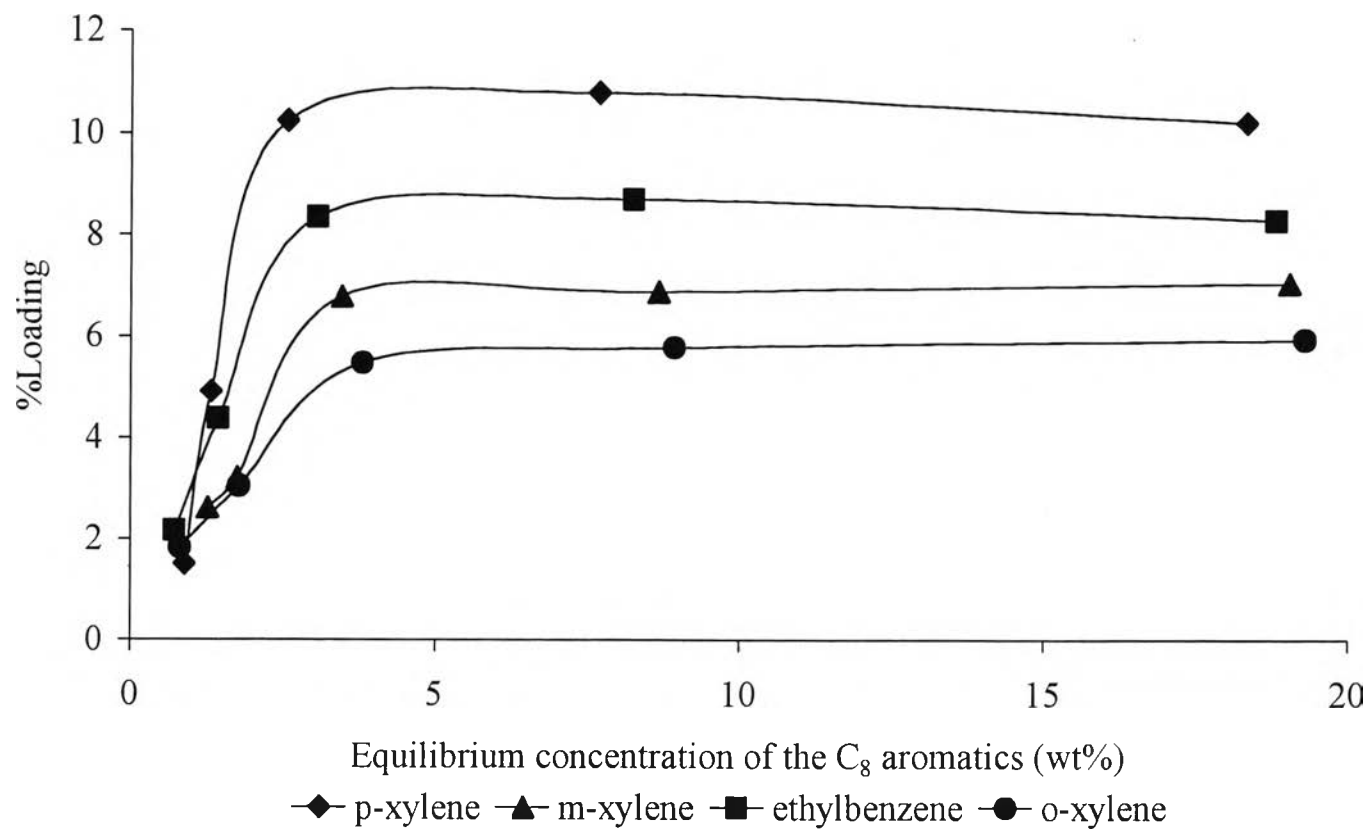
Figure 4.4 Adsorption of the C_8 aromatics on the *KY* zeolite at 40°C.
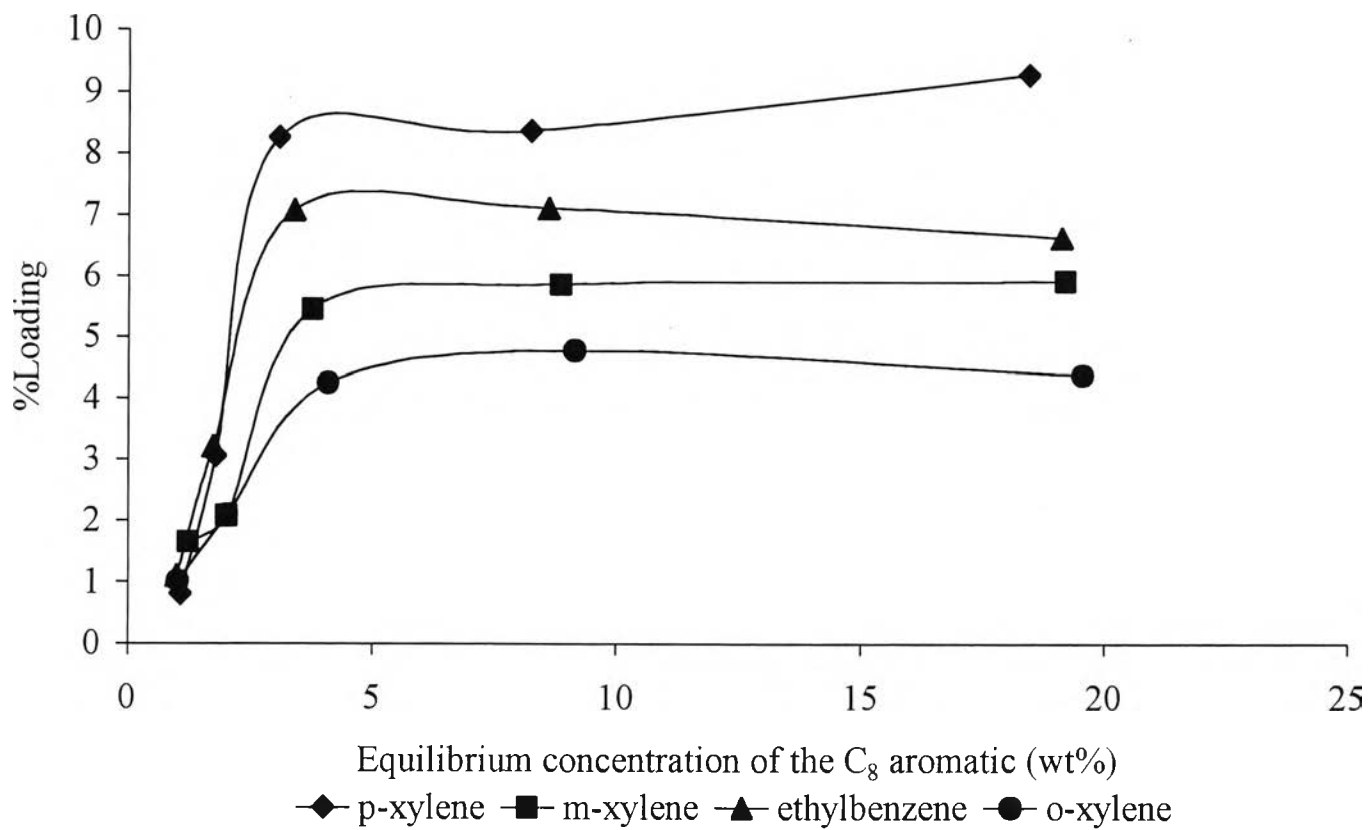
Figure 4.5 Adsorption of the C_8 aromatics on the *KY* zeolite at 65°C
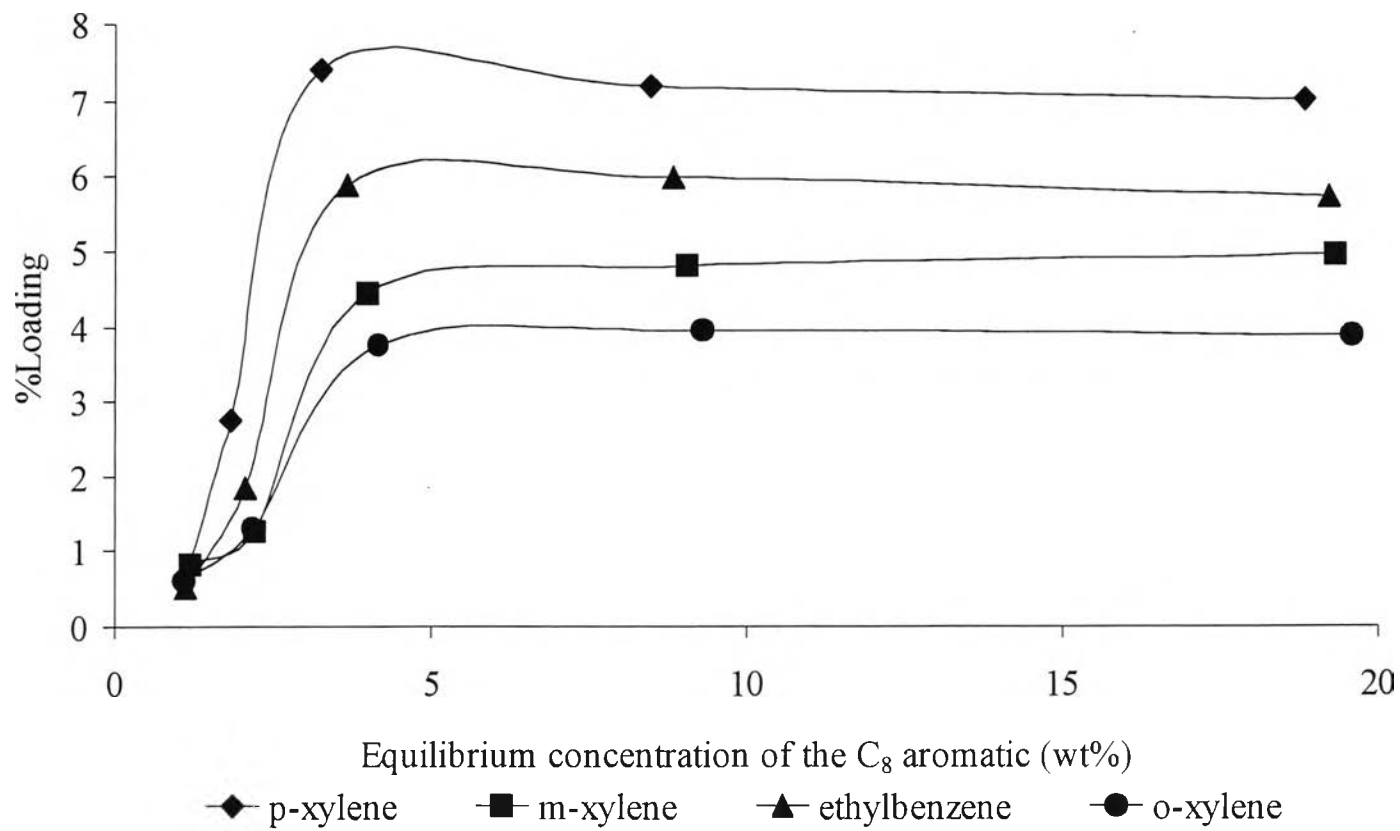
Figure 4.6 Adsorption of the C$_8$ aromatics on the *KY* zeolite at 90°C
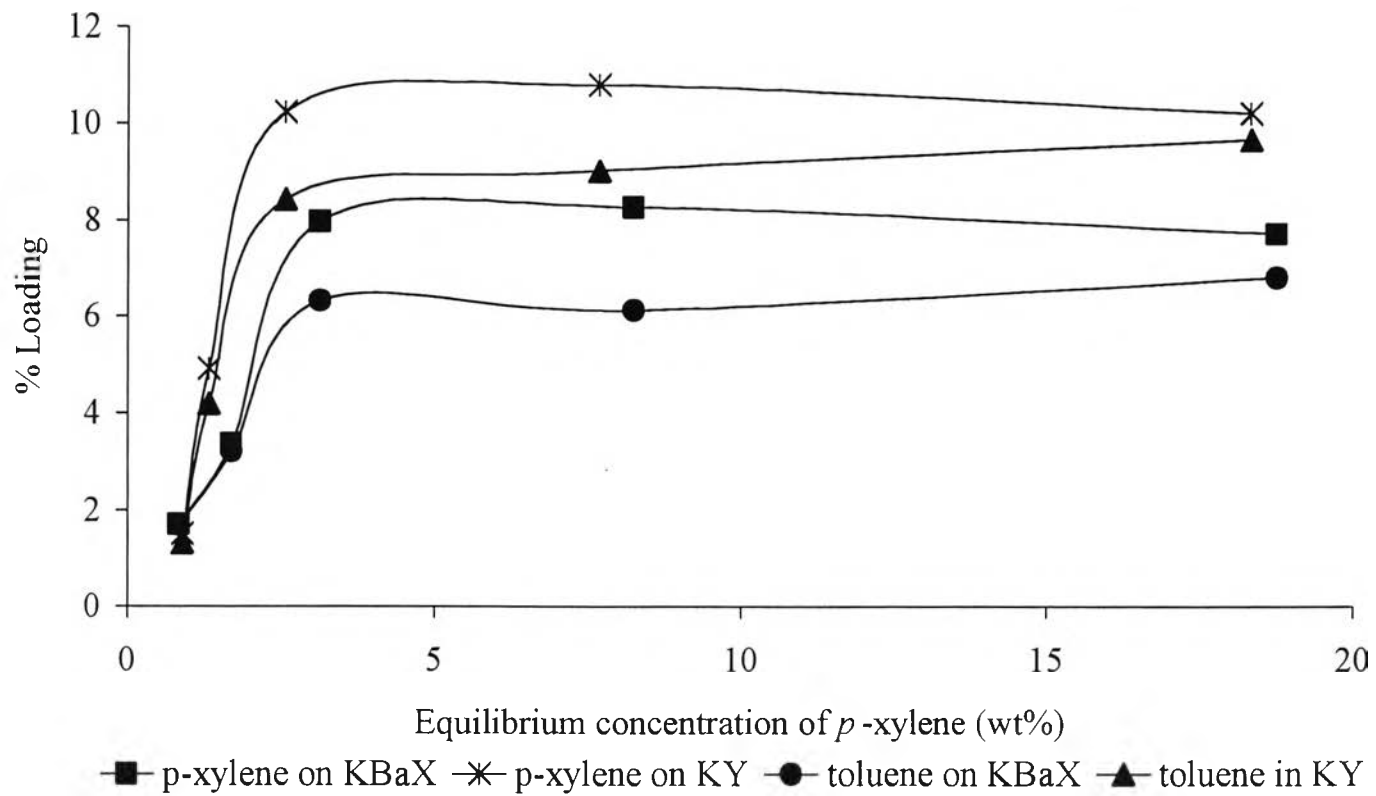
Figure 4.7 Adsorption of *p*-xylene and toluene on the *KBaX* and *KY* zeolites at 40°C.
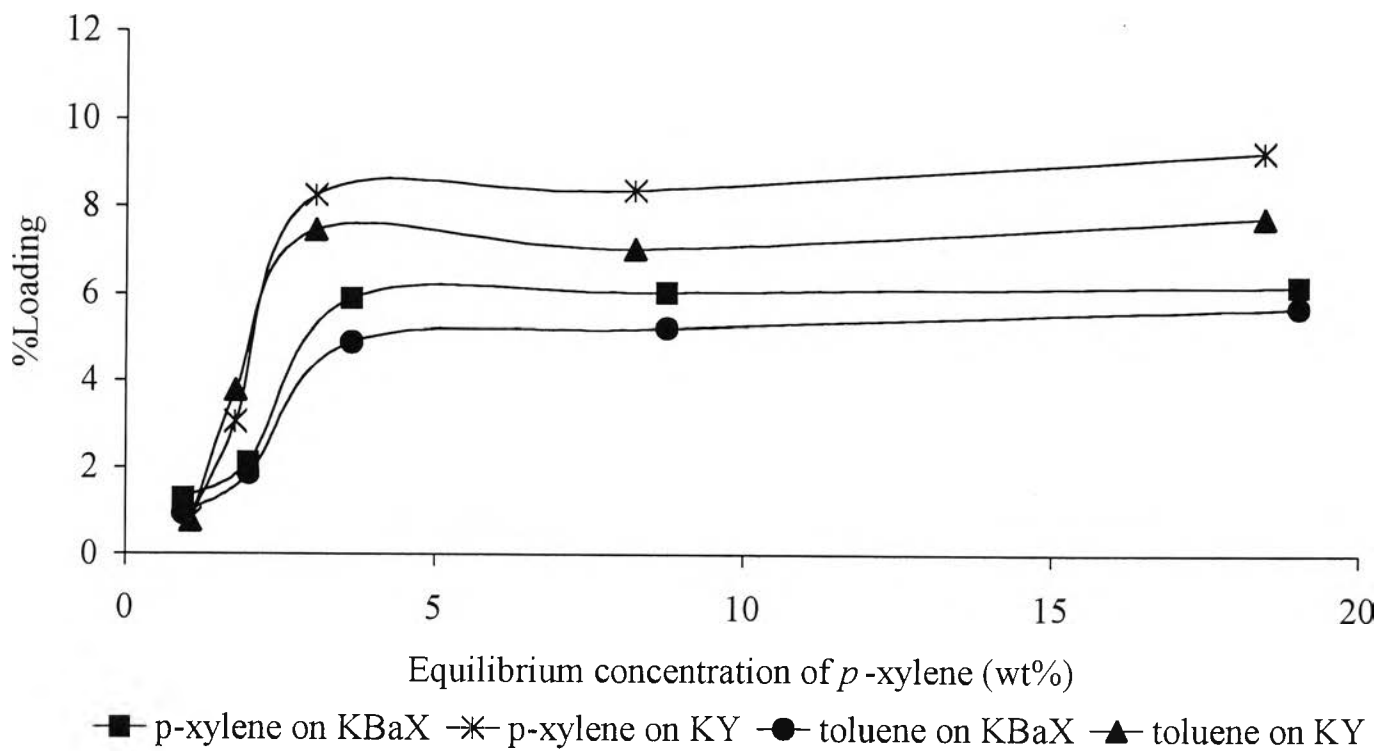
Figure 4.8 Adsorption of p-xylene and toluene on the *KBaX* and *KY* zeolites at 65°C.
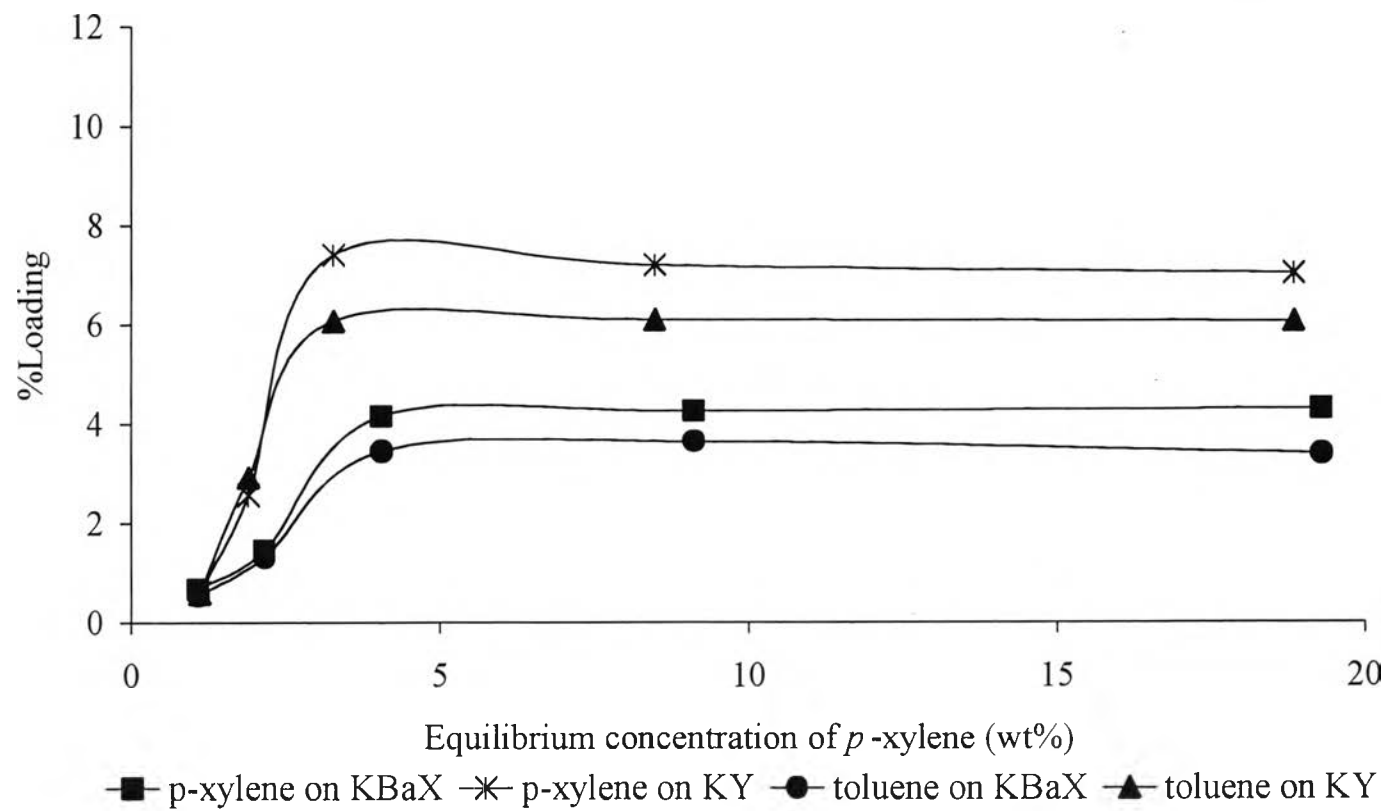
Figure 4.9 Adsorption of *p*-xylene and toluene on the *KBaX* and *KY* zeolites at 90°C.
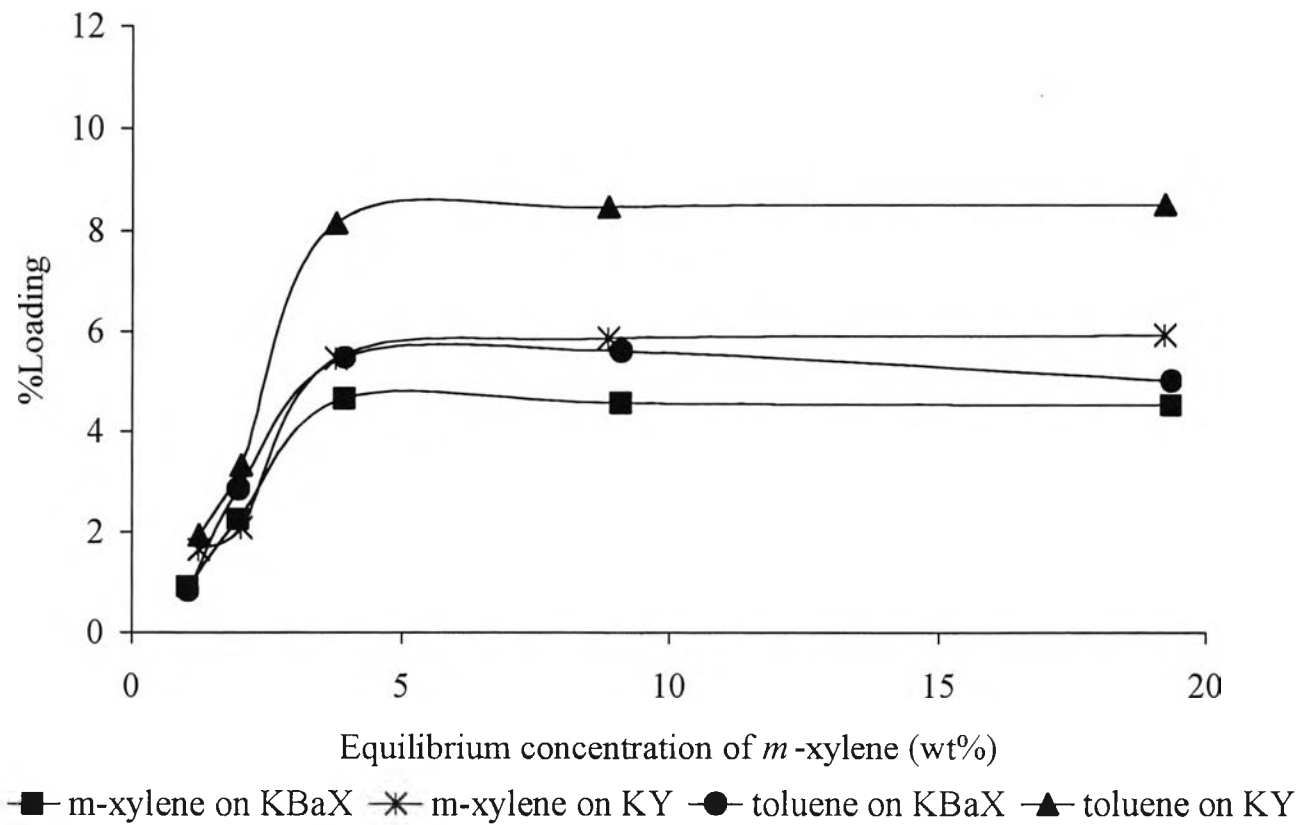
Figure 4.10 Adsorption of *m*-xylene and toluene on the *KBaX* and *KY* zeolites at 40°C.
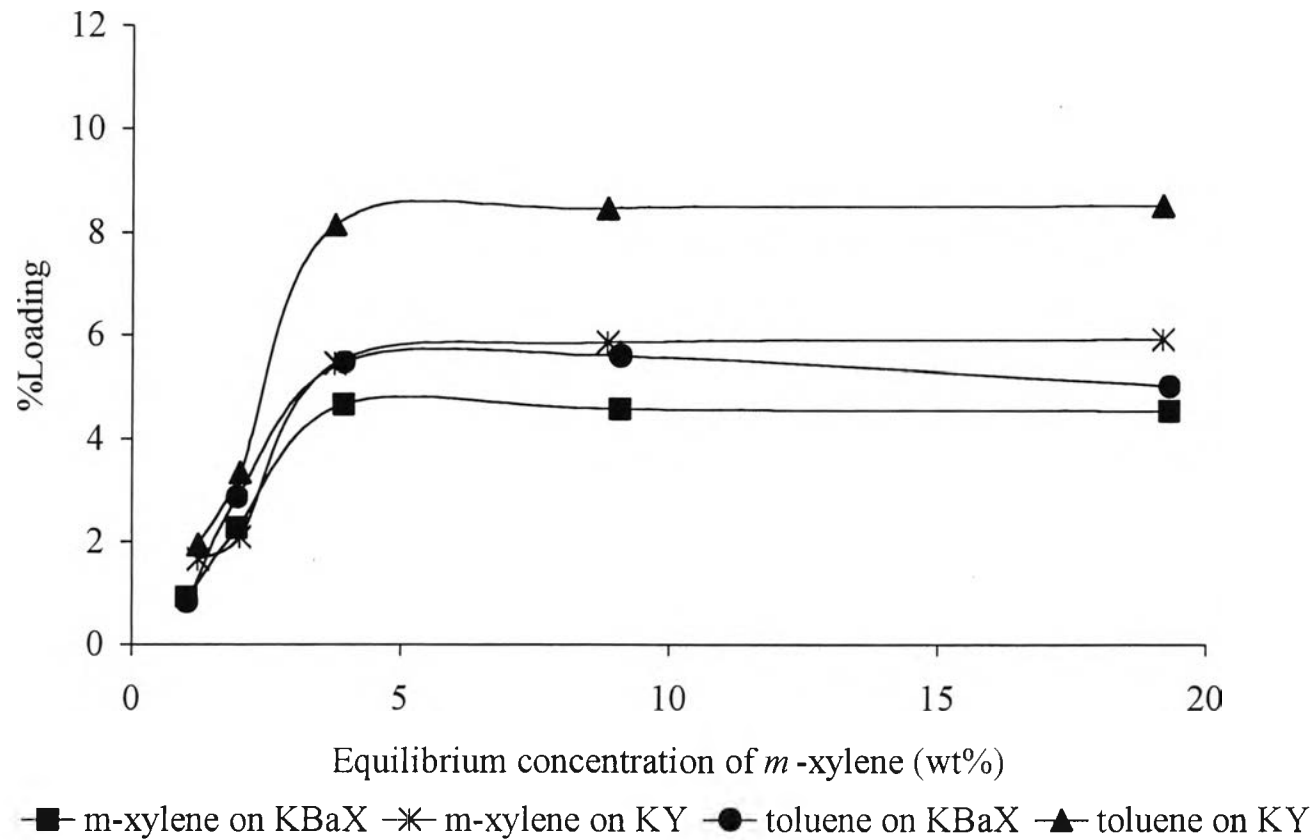
Figure 4.11 Adsorption of *m*-xylene and toluene on the *KBaX* and *KY* zeolites at 65°C.
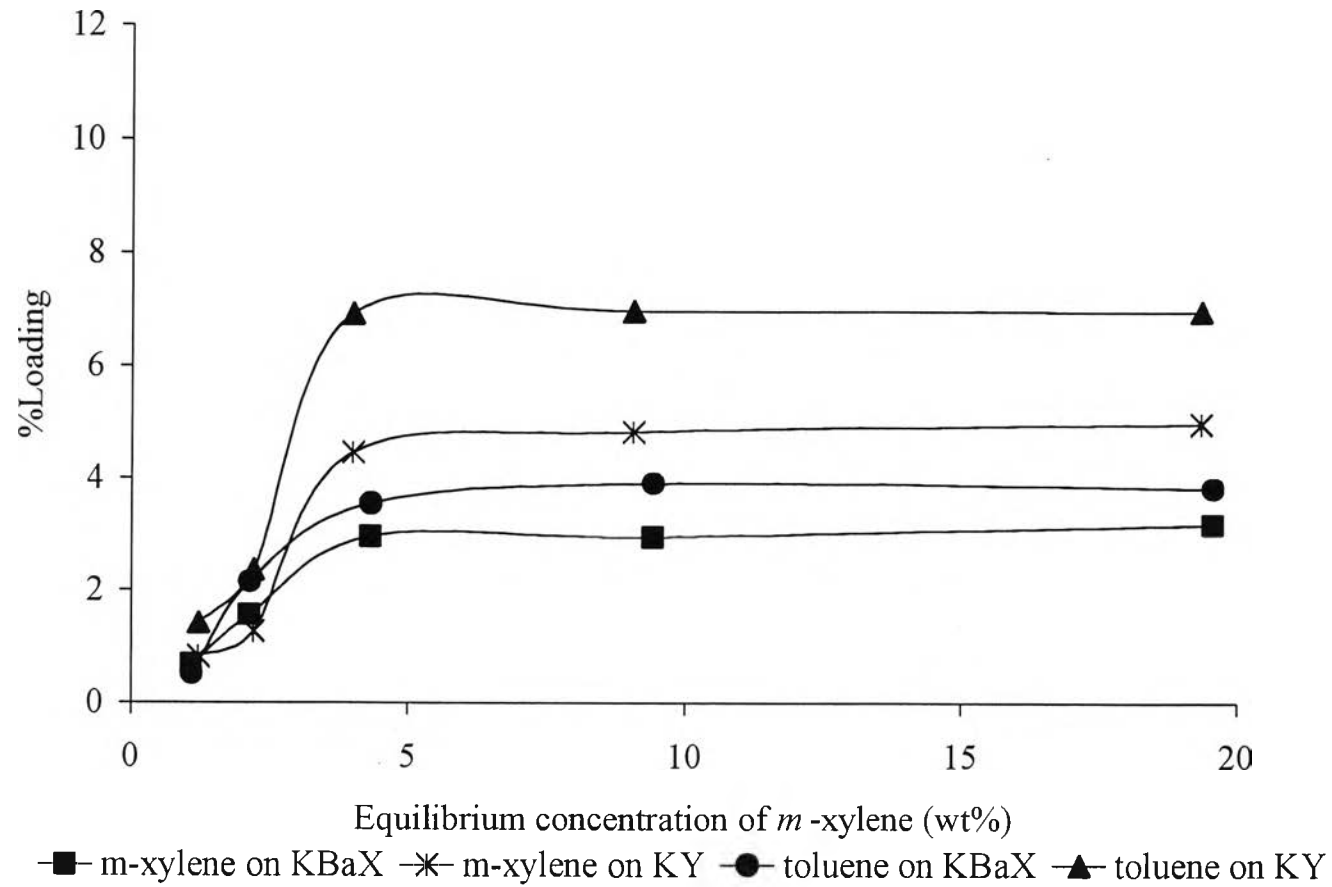
Figure 4.12 Adsorption of *m*-xylene and toluene on the *KBaX* and *KY* zeolites at 90°C.
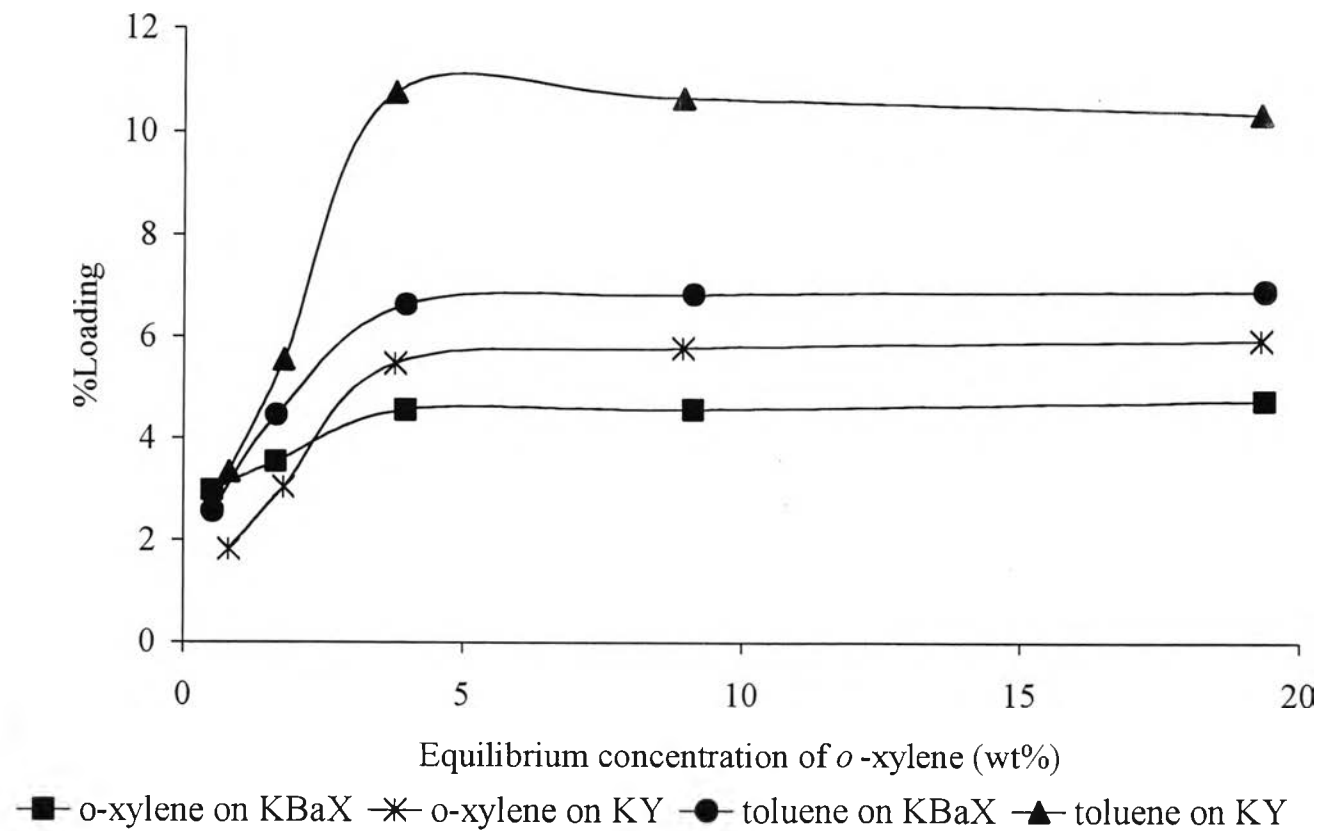
Figure 4.13 Adsorption of *o*-xylene and toluene on the *KBaX* and *KY* zeolites at 40°C.
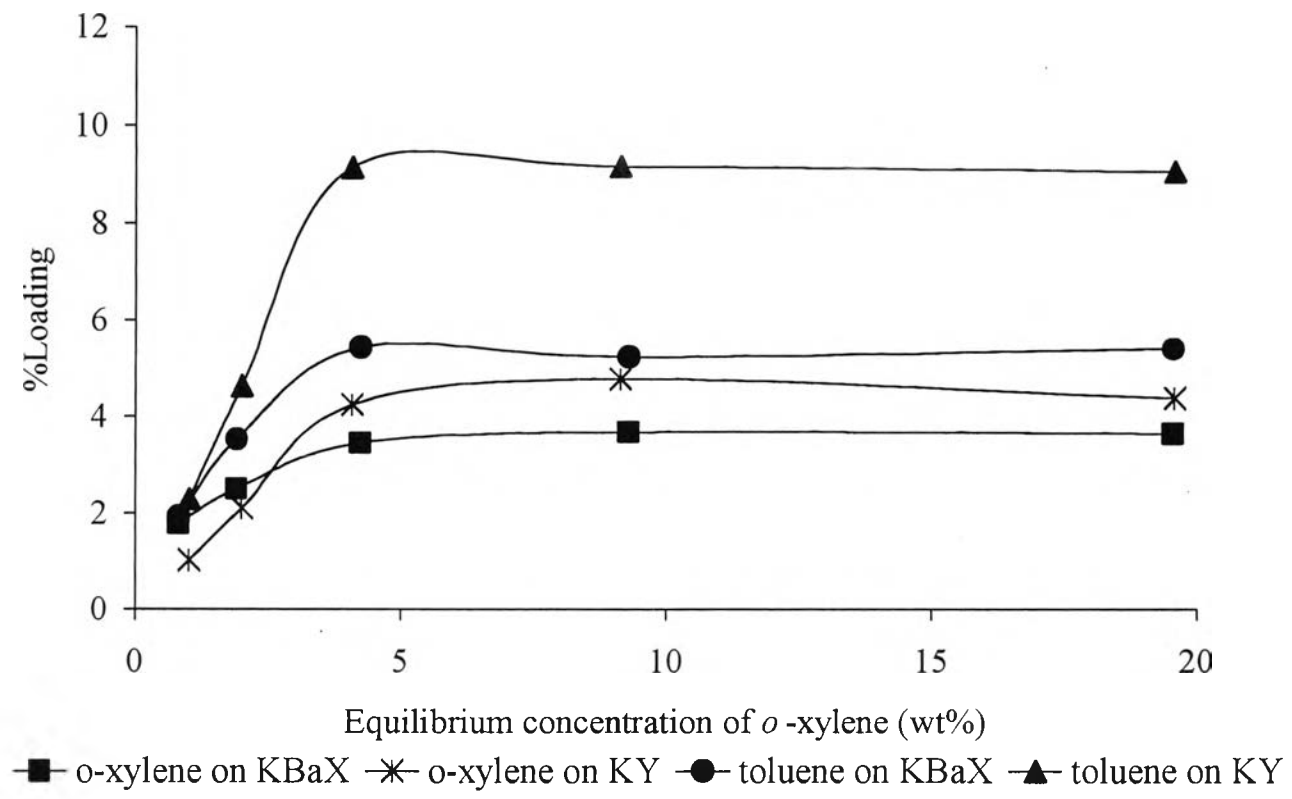
Figure 4.14 Adsorption of *o*-xylene and toluene on the *KBaX* and *KY* zeolites at 65°C.
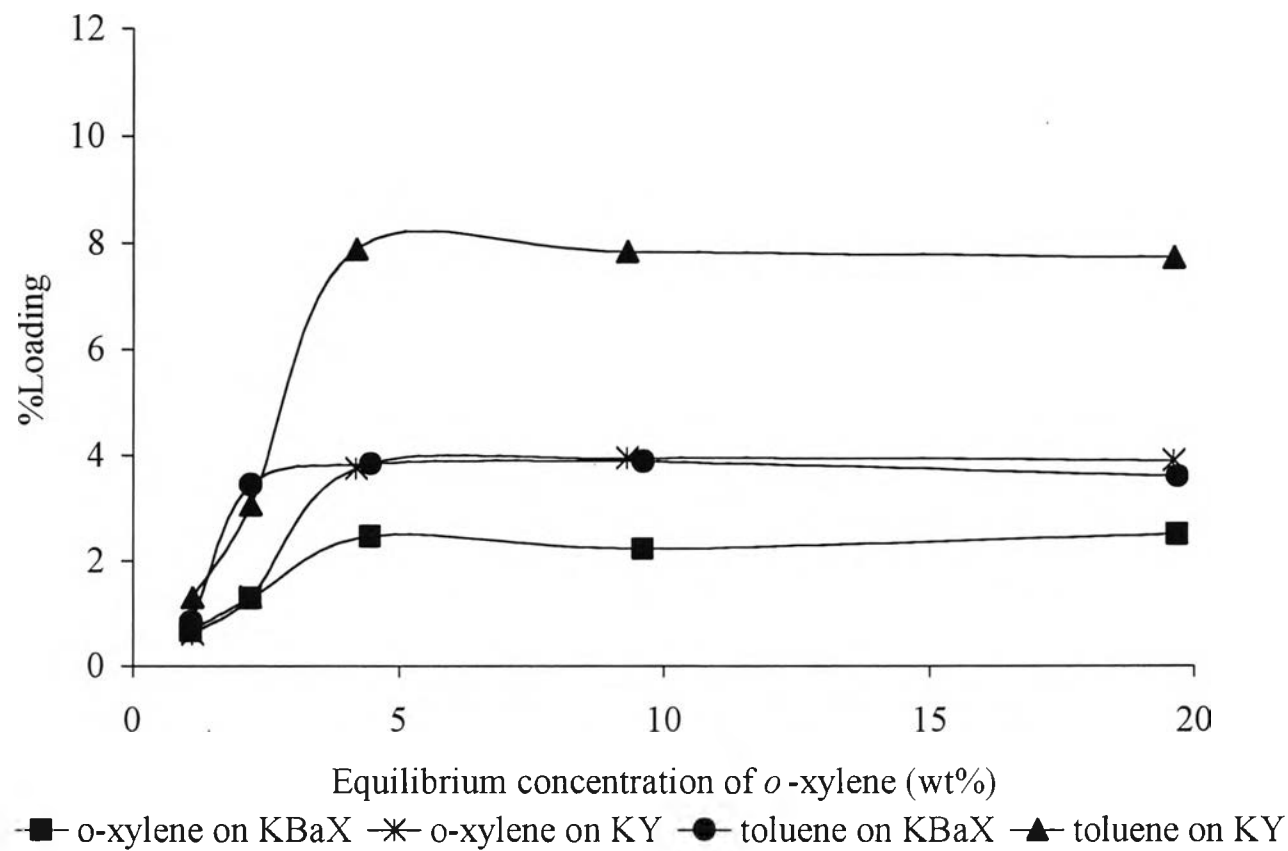
Figure 4.15 Adsorption of *o*-xylene and toluene on the *KBaX* and *KY* zeolites at 90°C.
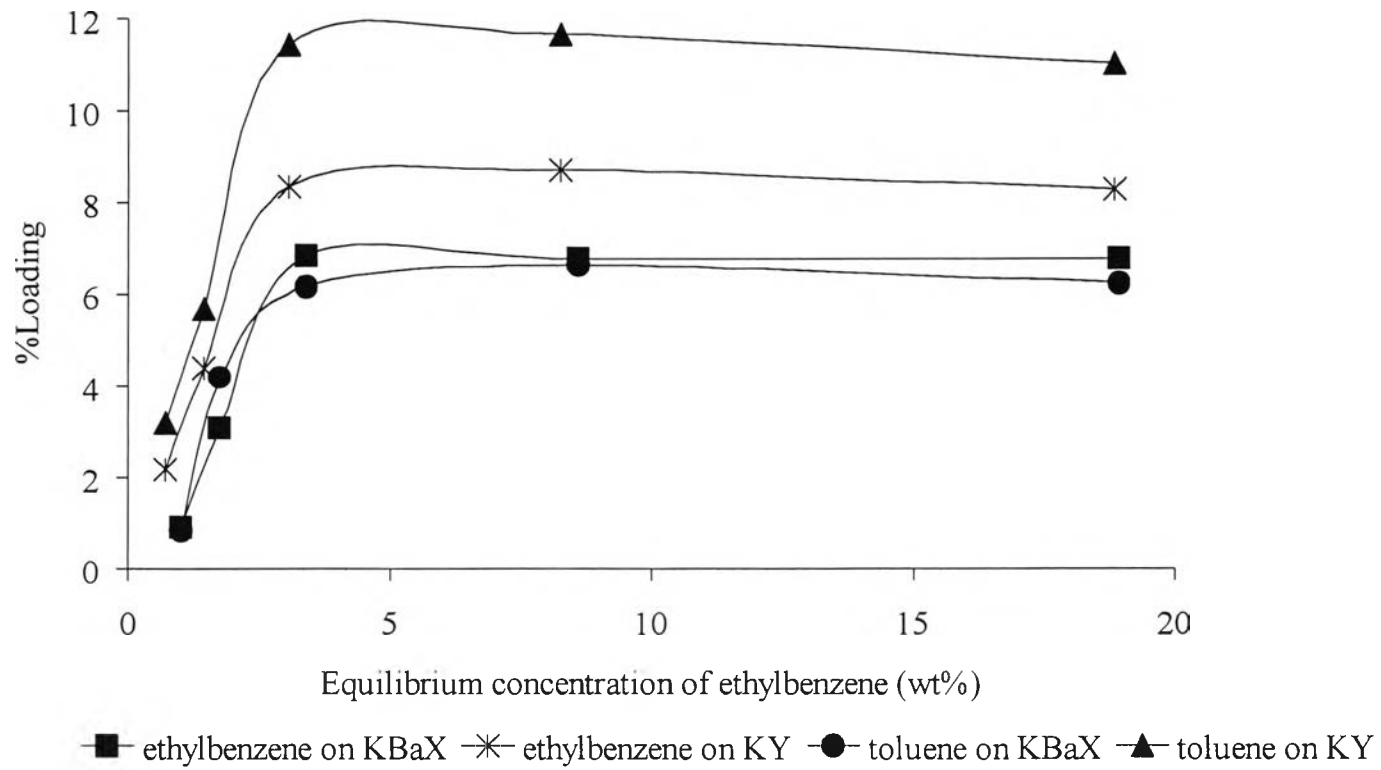
Figure 4.16 Adsorption at ethylbenzene and toluene on the *KBaX* and *KY* zeolites at 40°C
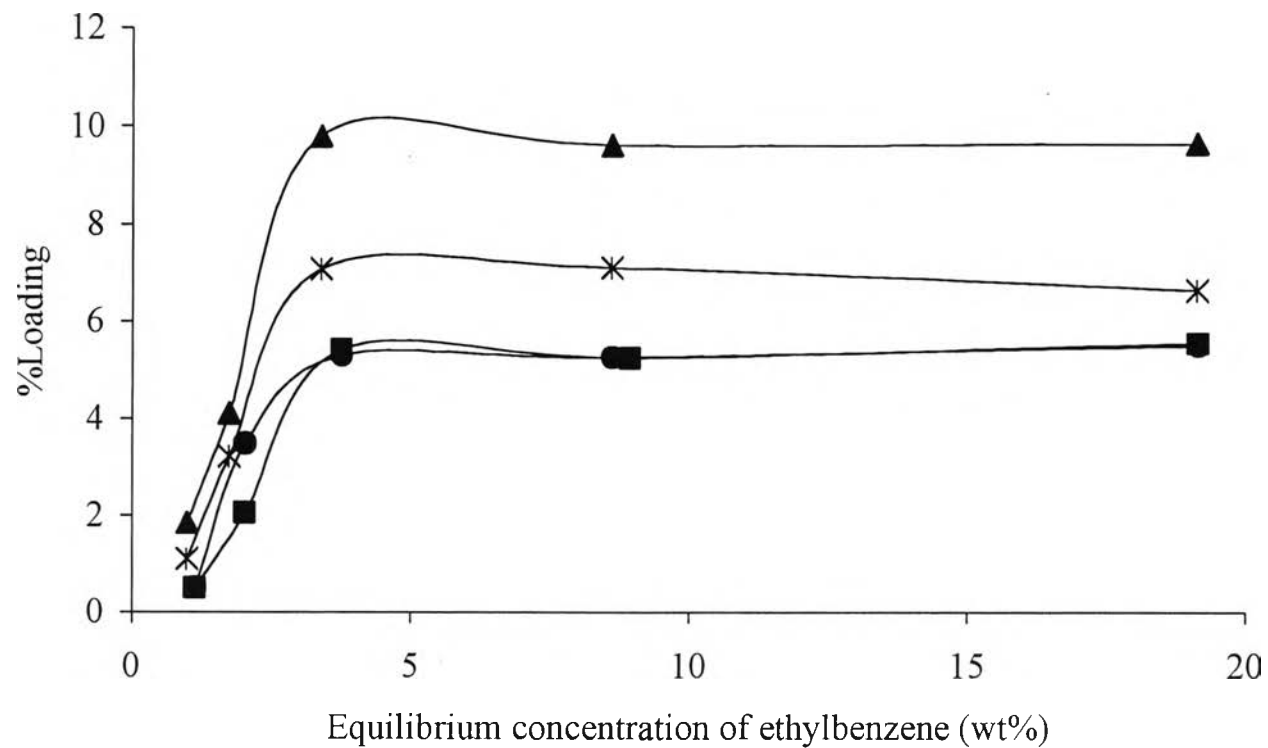
Figure 4.17 Adsorption of ethylbenzene and toluene on the *KBaX* and *KY* zeolites at 65°C.
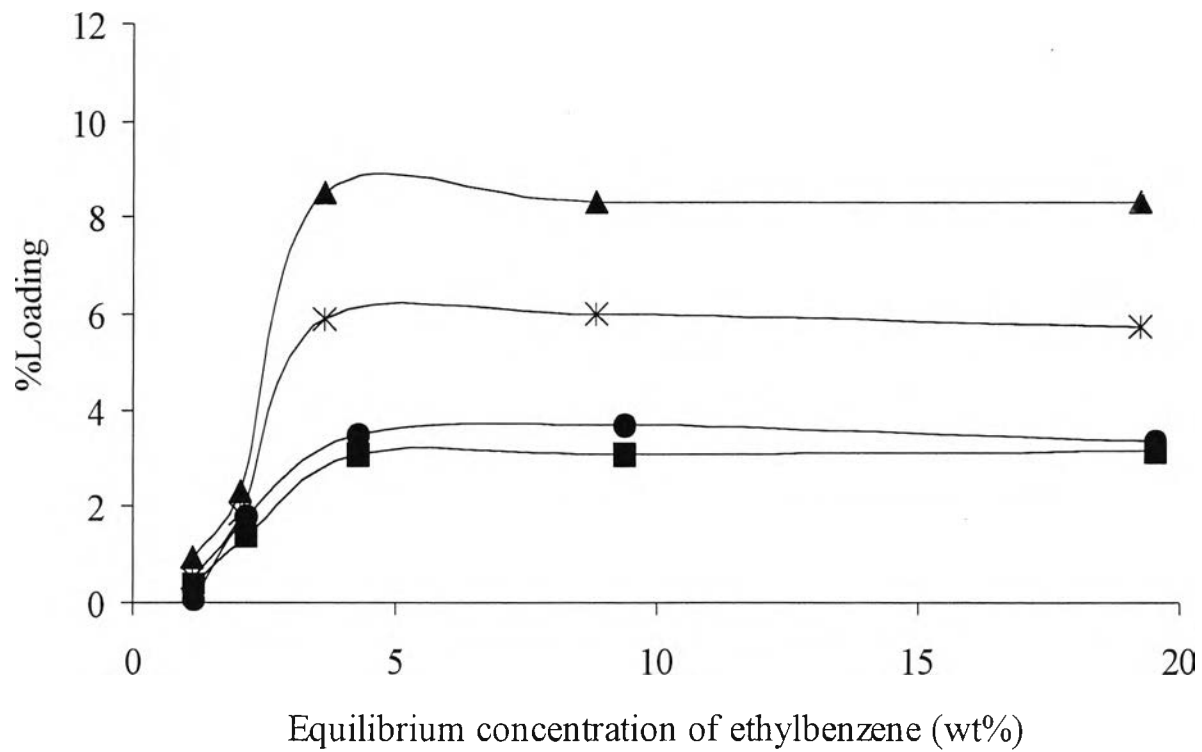
Figure 4.18 Adsorption at ethylbenzene and toluene on the *KBaX* and *KY* zeolites at 90°C.
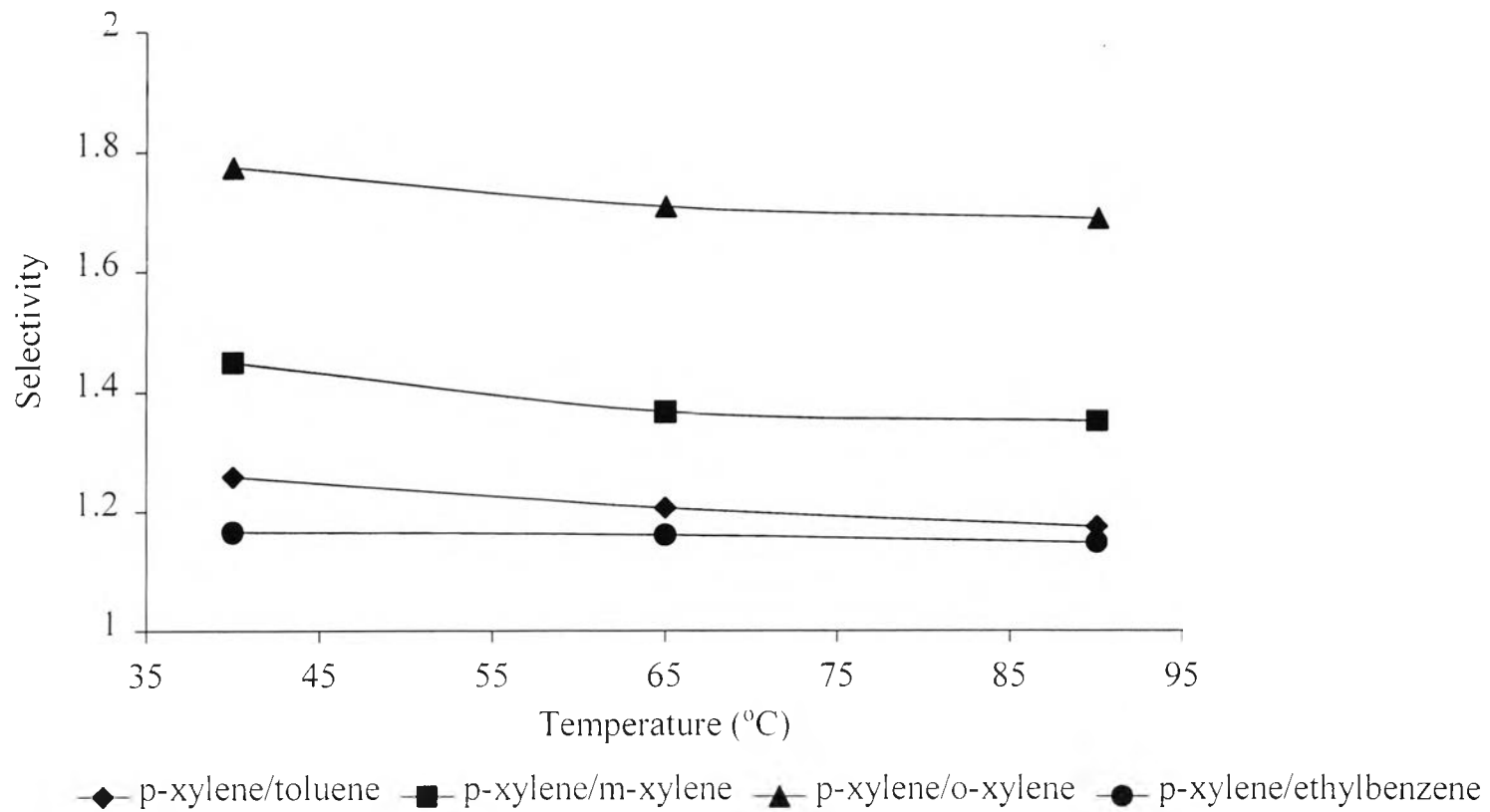
Figure 4.19 Selectivity of *p*-xylene from other C_8 aromatics and toluene on the *KBaX* zeolite.
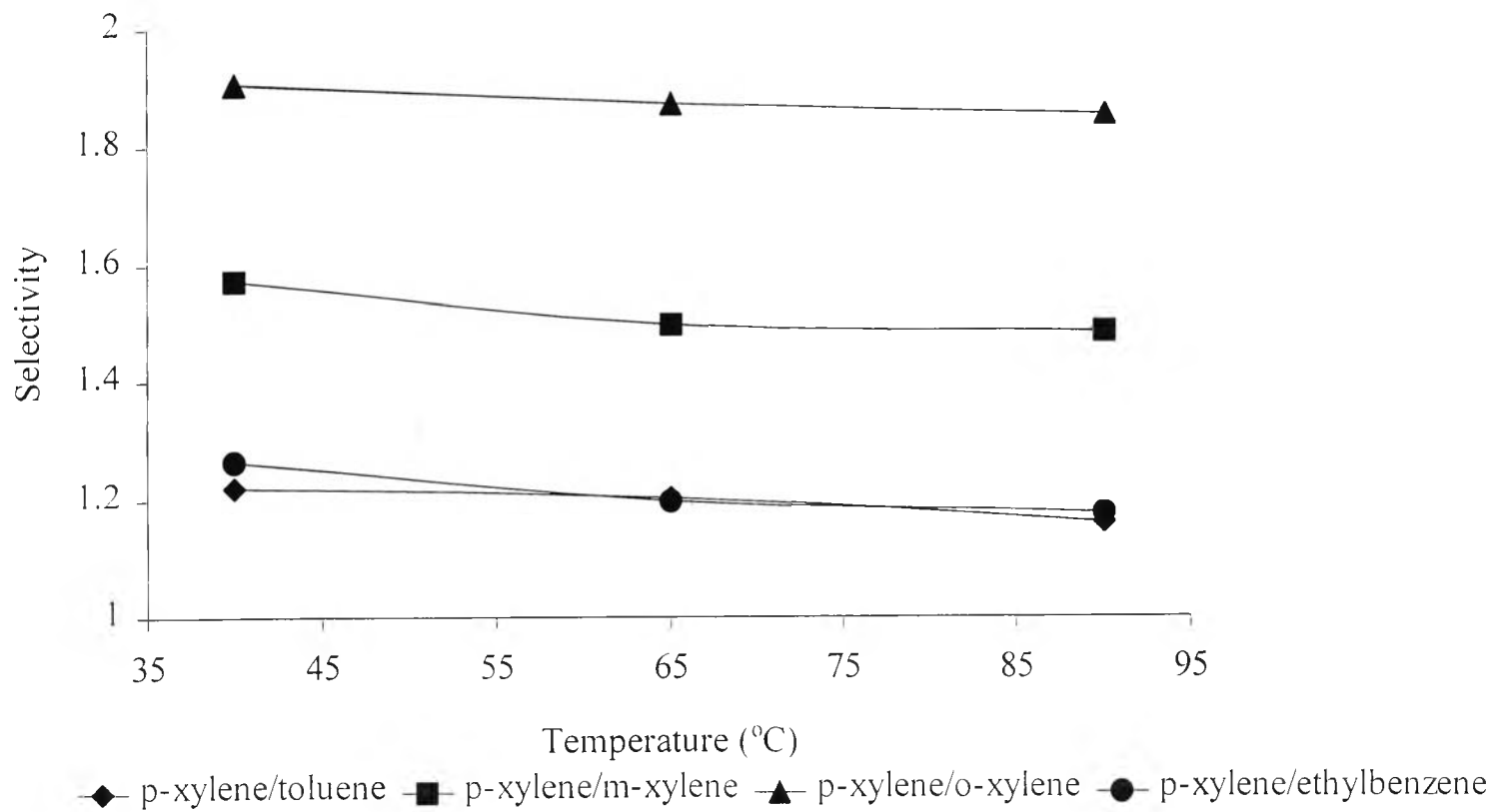
Figure 4.20 Selectivity of p-xylene from other C_8aromatics and toluene on the KY zeolite.
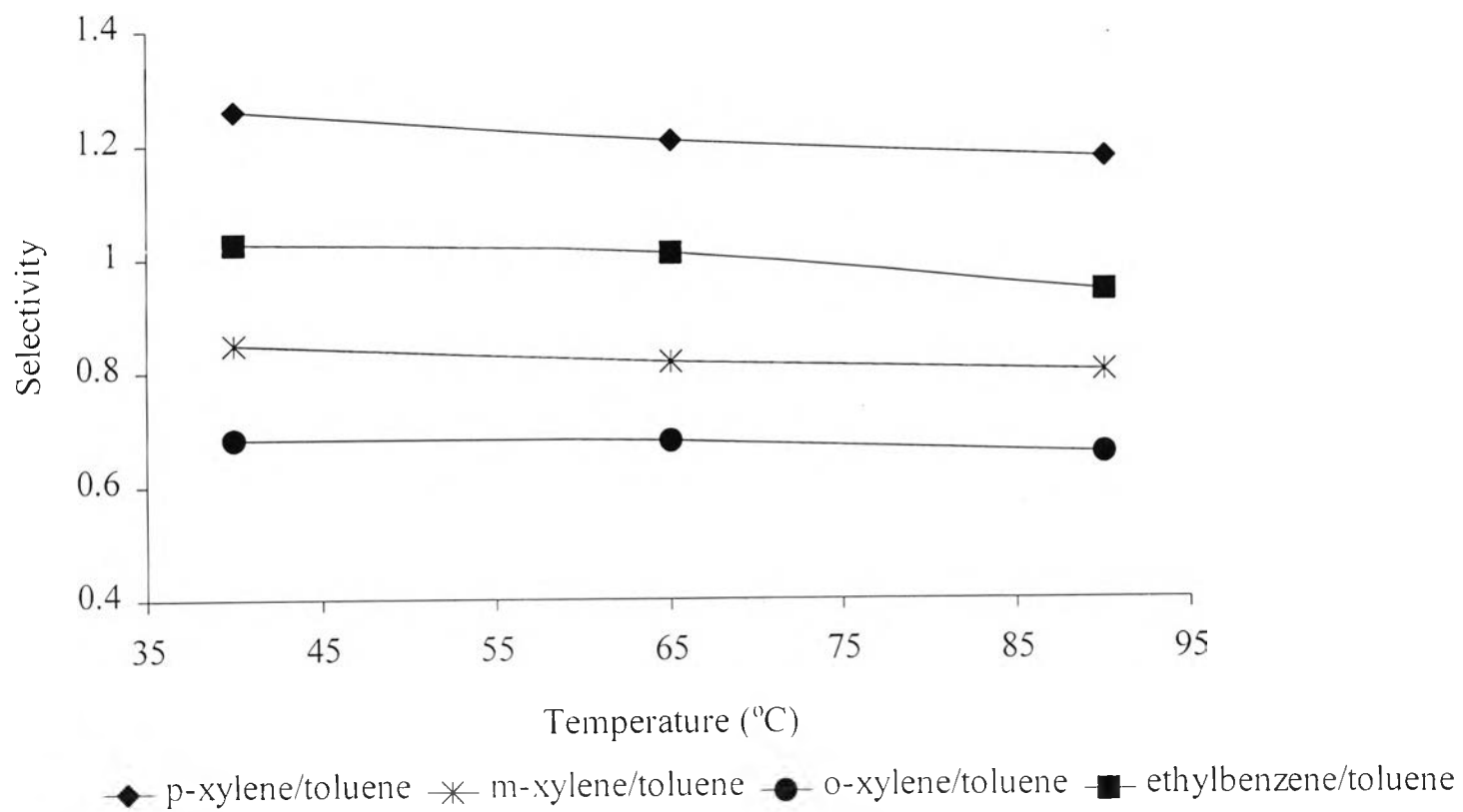
Figure 4.21 Selectivity of the C$_8$ aromatics from toluene on the *KBaX* zeolite.
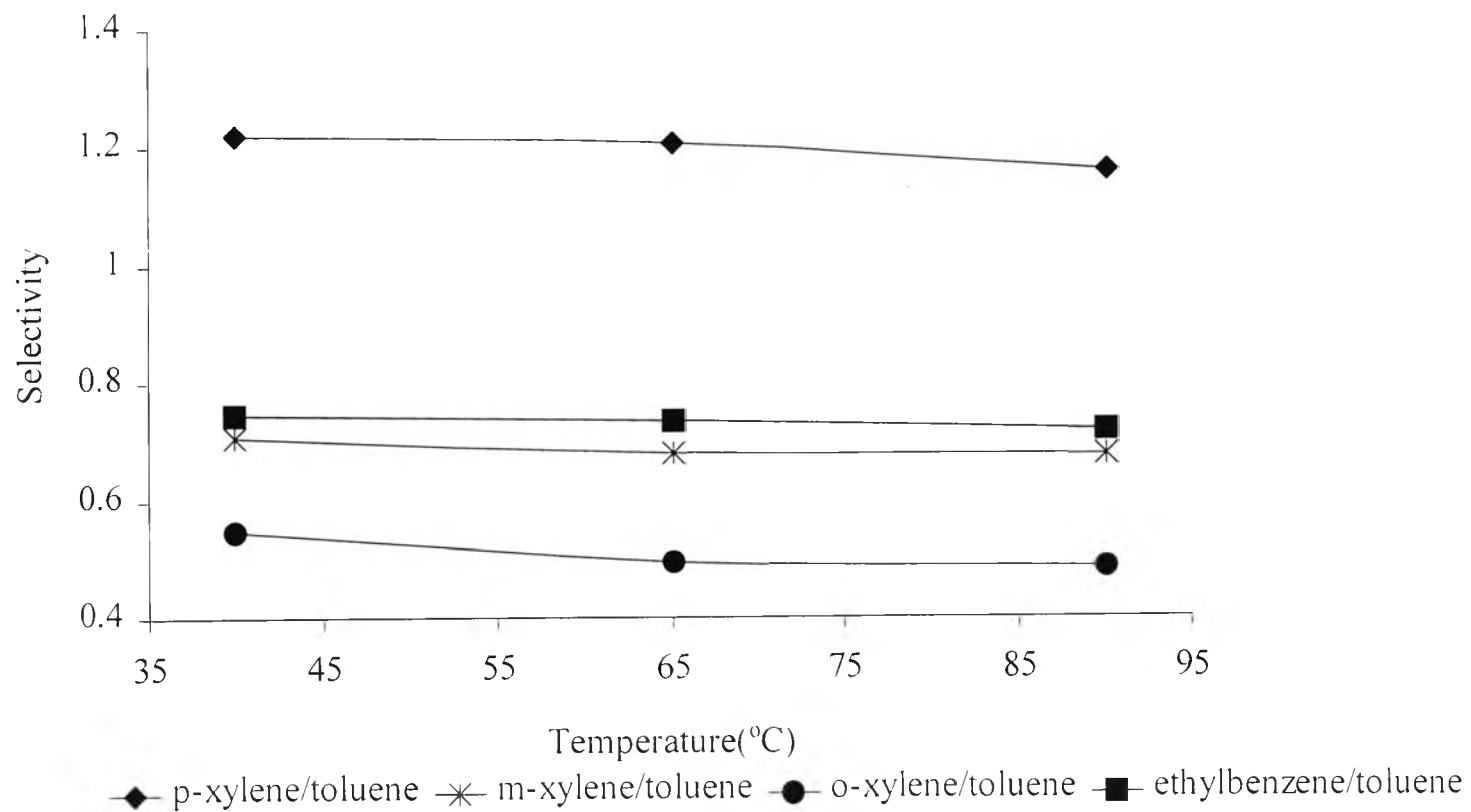
Figure 4.22 Selectivity of the C_8 aromatics from toluene on the KY zeolite.
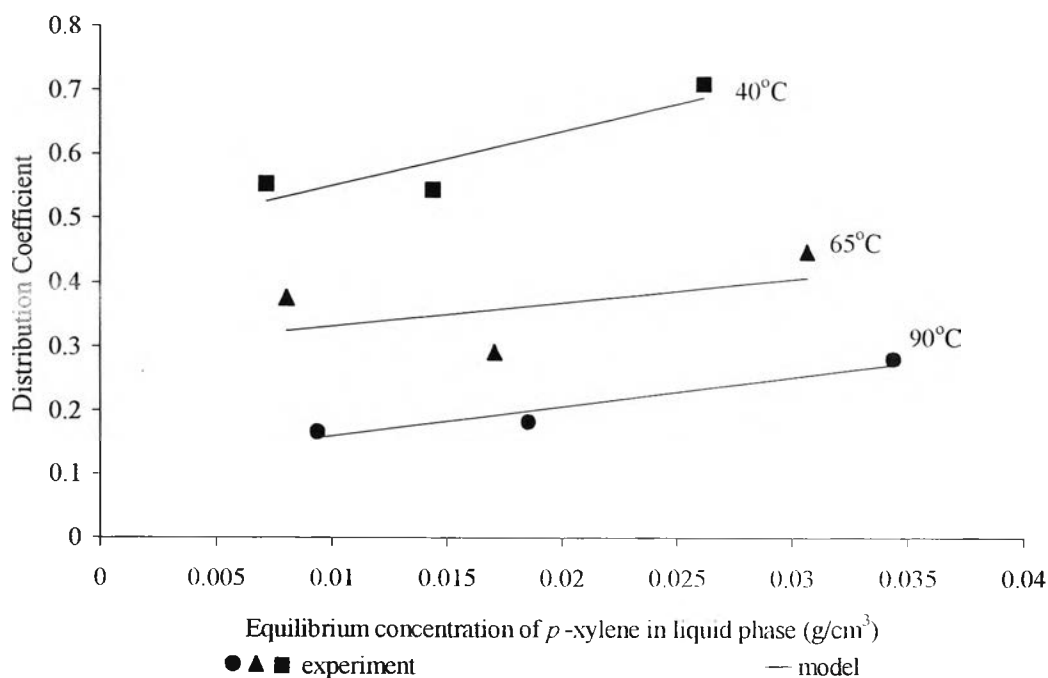
Figure 4.23 Comparison of experimental data and model prediction of *p*-xylene on the *KBaX* zeolite in *p*-xylene/toluene at 40, 65 and 90°C.
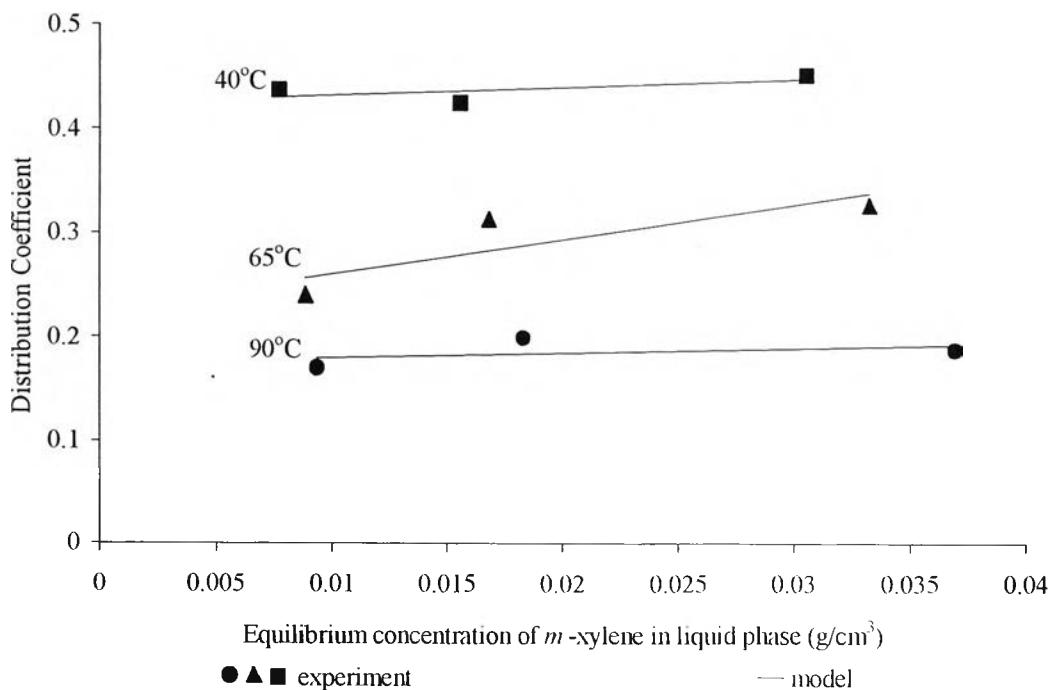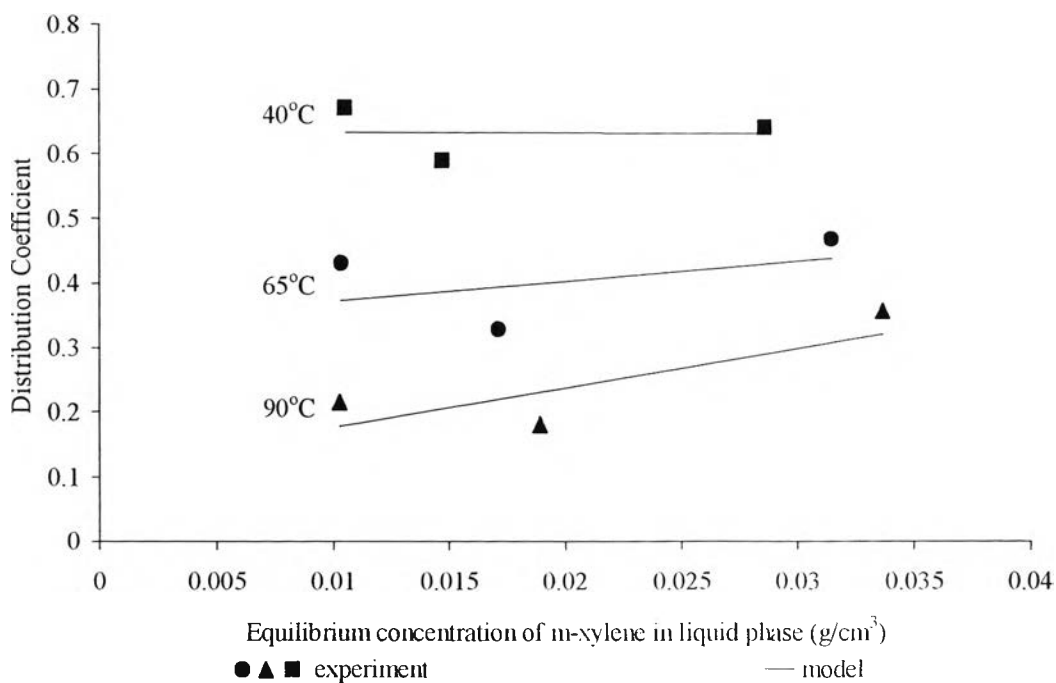

Figure 4.24 Comparison of experimental data and model prediction of *m*-xylene on the *KBaX* zeolite in *m*-xylene/toluene at 40, 65 and 90°C.
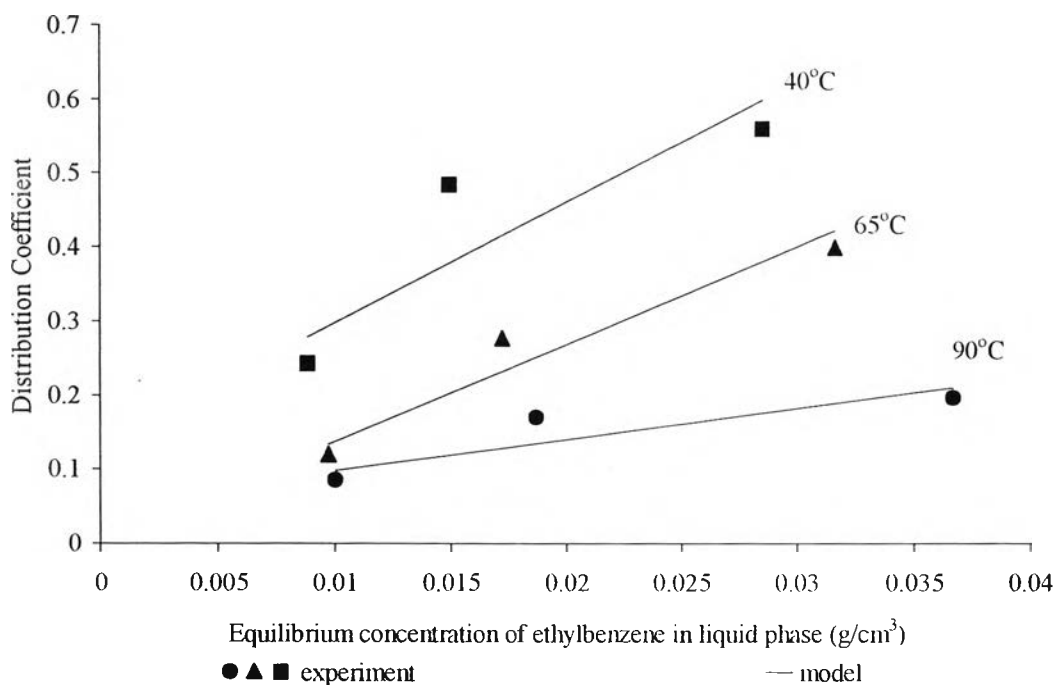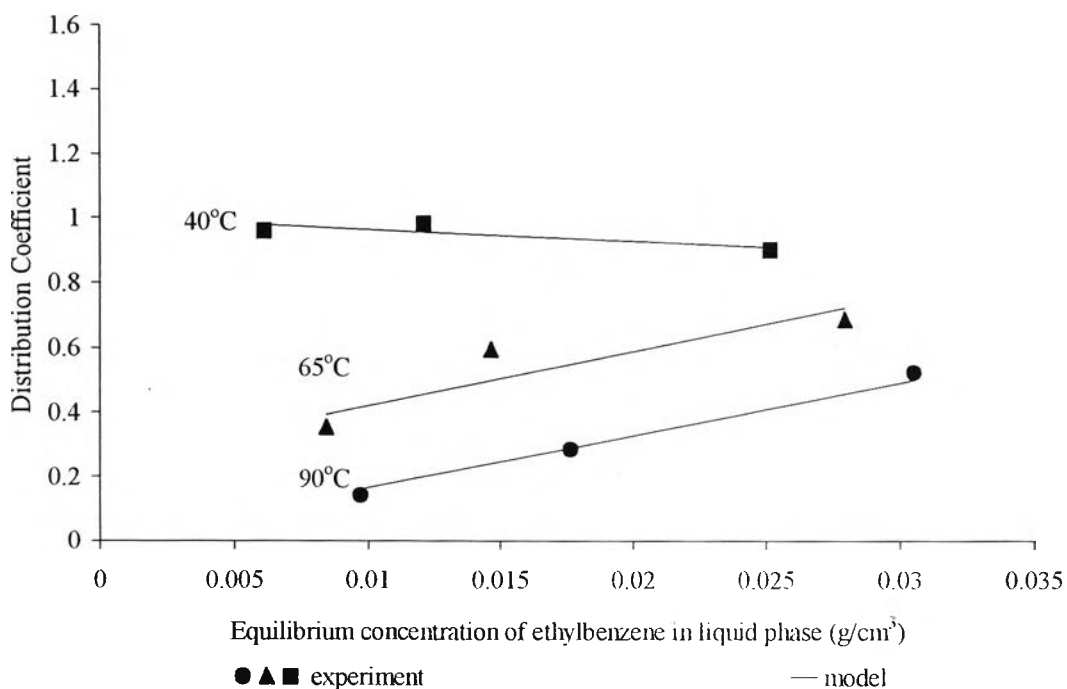
Figure 4.25 Comparison of experimental data and model prediction of ethylbenzene on the *KBaX* zeolite in ethylbenzene/toluene at 40, 65 and 90°C.
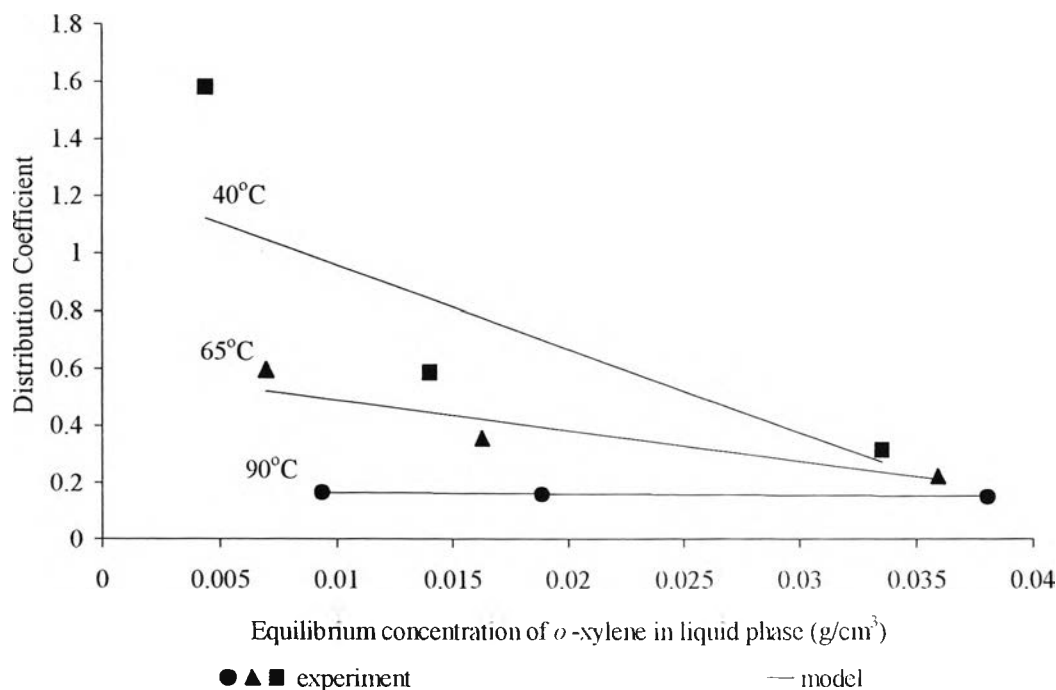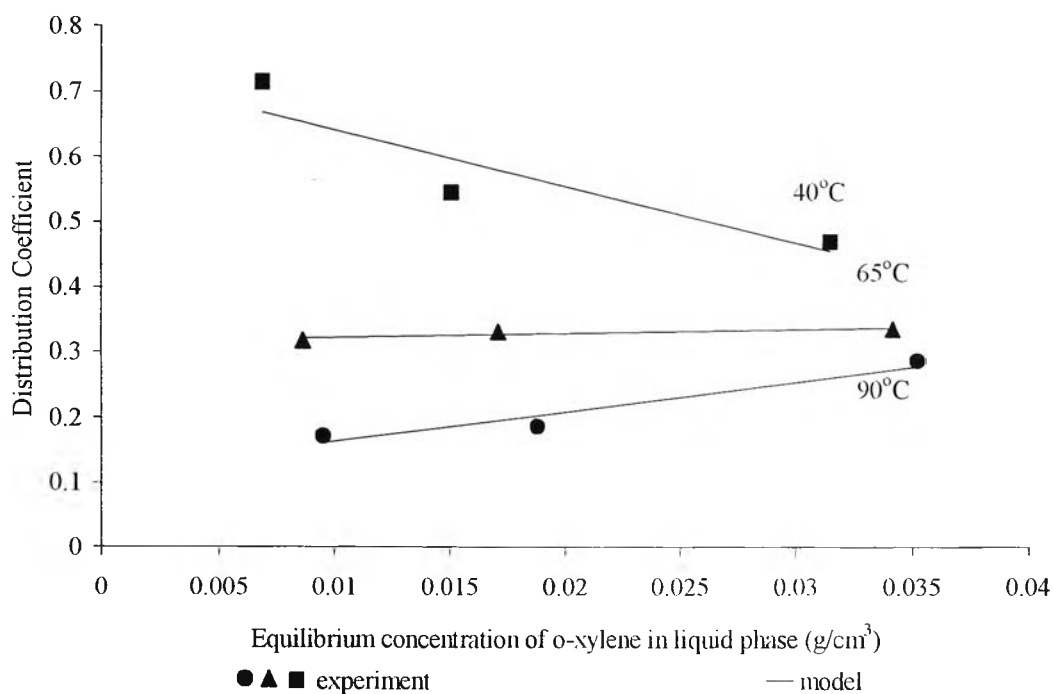

Figure 4.26 Comparison of experimental data and model prediction of *o*-xylene on the *KBaX* zeolite in *o*-xylene/toluene at 40, 65 and 90°C.
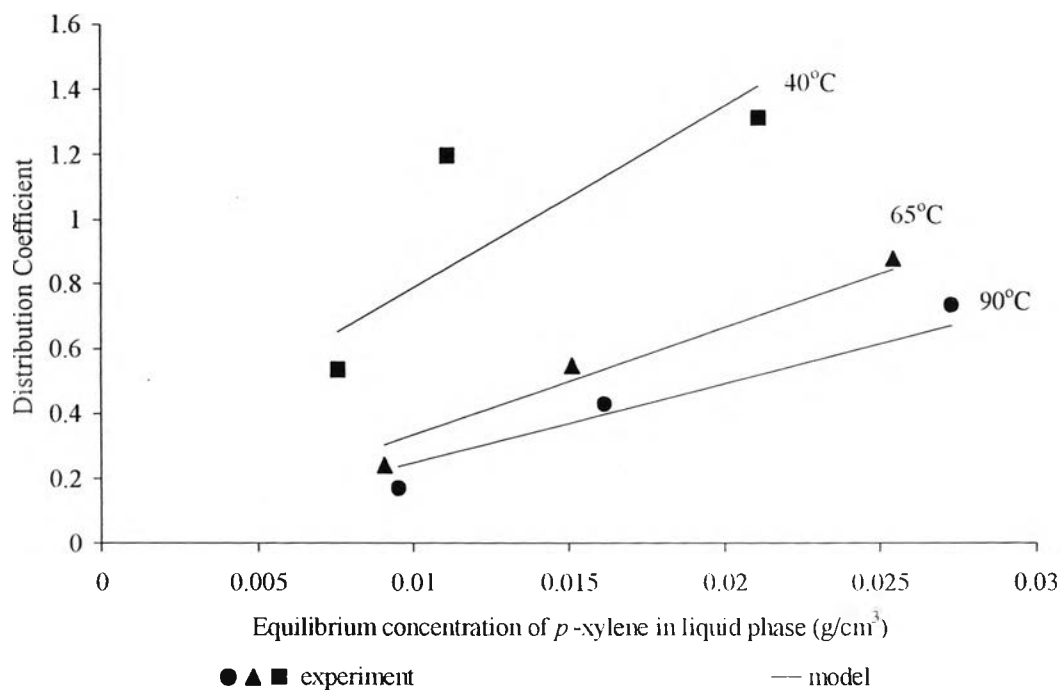
Figure 4.27 Comparison of experimental data and model prediction of *p*-xylene on the *KY* zeolite in *p*-xylene/toluene at 40, 65 and 90°C.
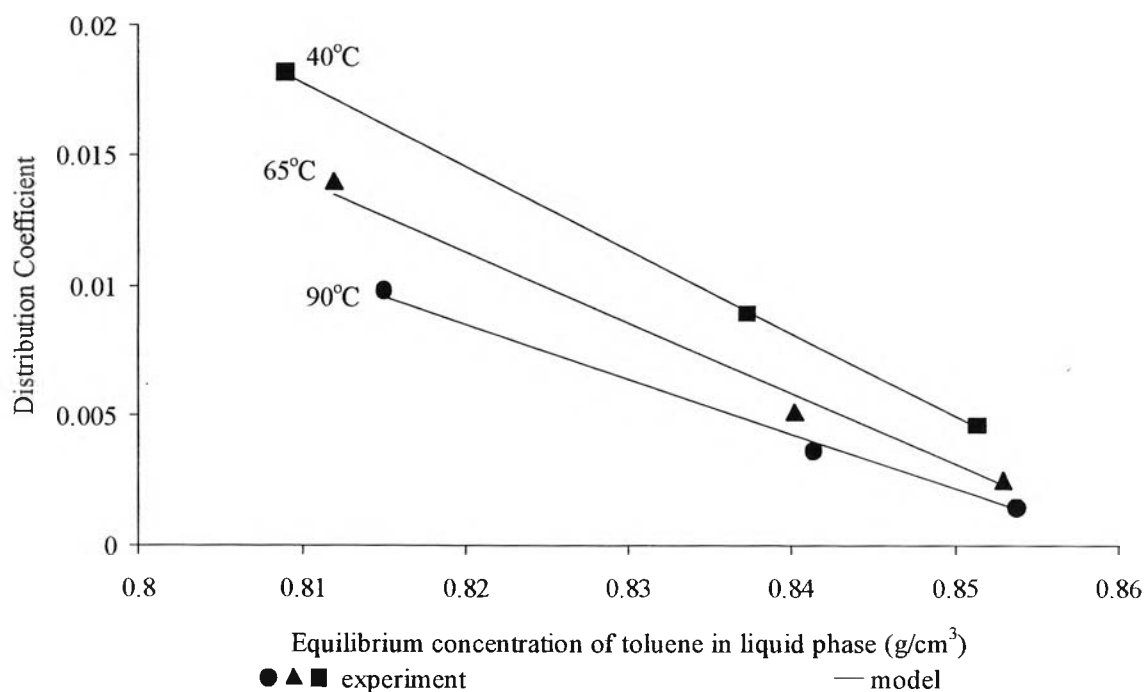

Figure 4.28 Comparison of experimental data and model prediction of *m*-xylene on the *KY* zeolite in *m*-xylene/toluene at 40, 65 and 90°C.

Figure 4.29 Comparison of experimental data and model prediction of ethylbenzene on the *KY* zeolite in ethylbenzene/toluene at 40, 65 and 90°C.

Figure 4.30 Comparison of experimental data and model prediction of *o*-xylene on the *KY* zeolite in *o*-xylene/toluene at 40, 65 and 90°C.

Figure 4.31 Comparison of experimental data and model prediction of toluene on the *KBaX* zeolite in *p*-xylene/toluene at 40, 65 and 90°C.
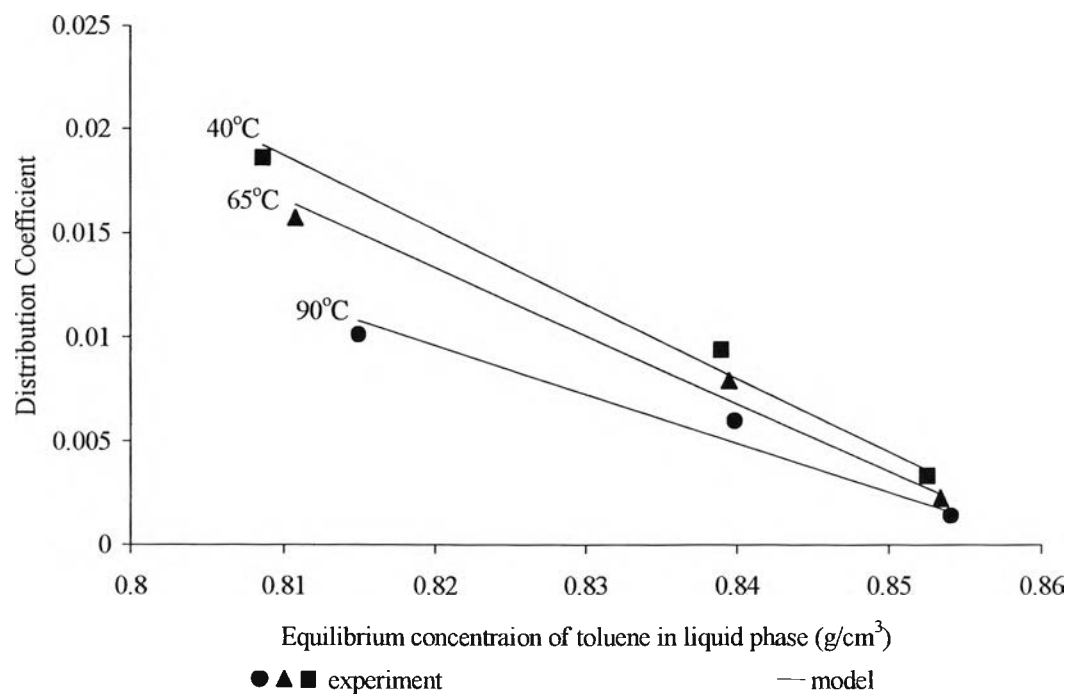

Figure 4.32 Comparison of experimental data and model prediction of toluene on the *KBaX* zeolite in *m*-xylene/toluene at 40, 65 and 90°C.
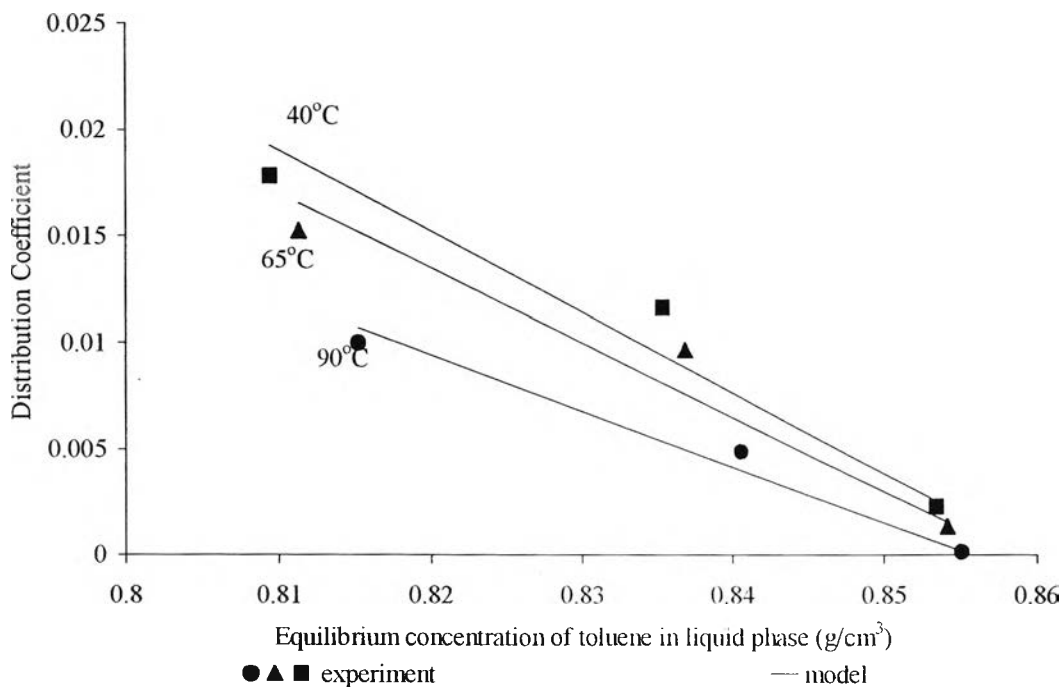
Figure 4.33 Comparison of experimental data and model prediction of toluene on the *KBaX* zeolite in ethylbenzene /toluene at 40, 65 and 90°C.
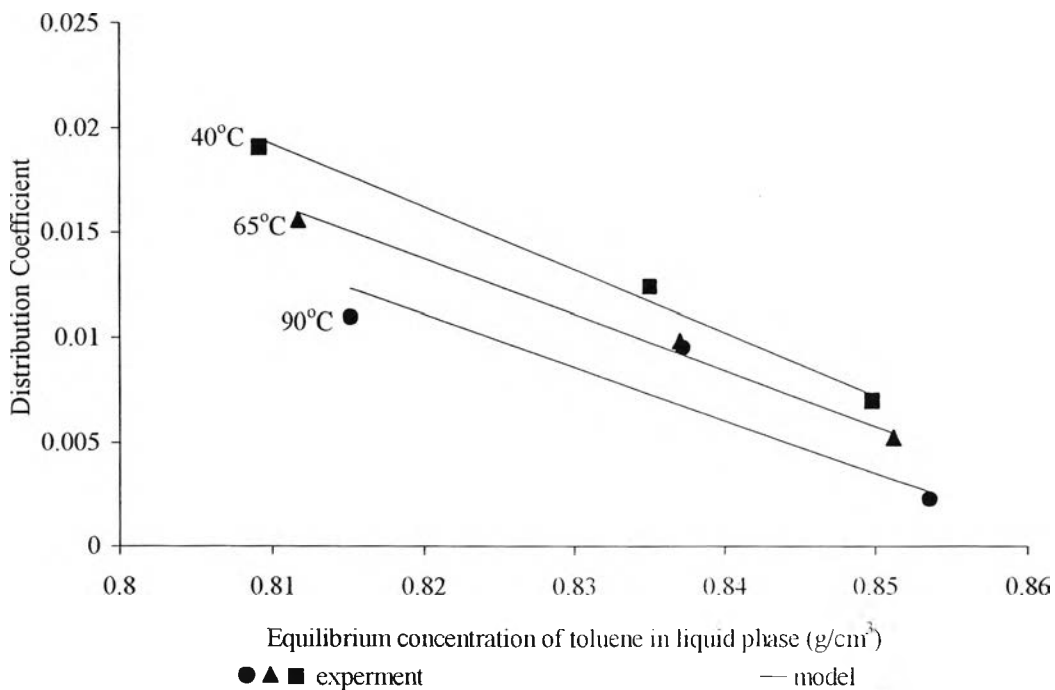

Figure 4.34 Comparison of experimental data and model prediction of toluene on the *KBaX* zeolite in *o*-xylene /toluene at 40, 65 and 90°C.
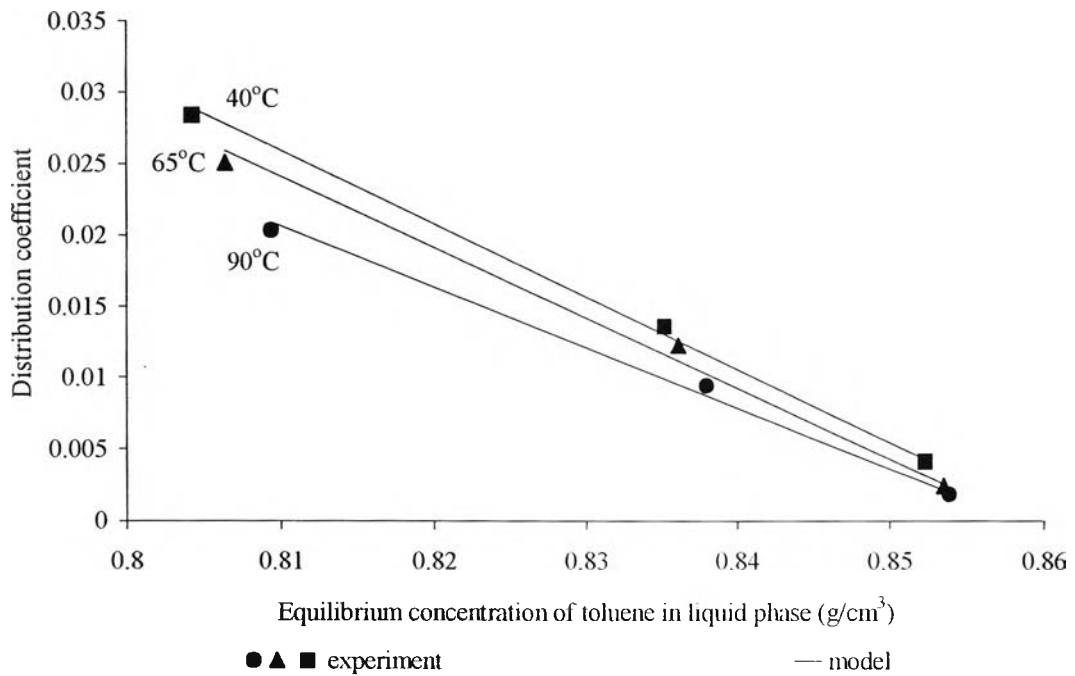
Figure 4.35 Comparison of experimental data and model prediction of toluene on the *KY* zeolite in *p*-xylene /toluene at 40, 65 and 90°C.
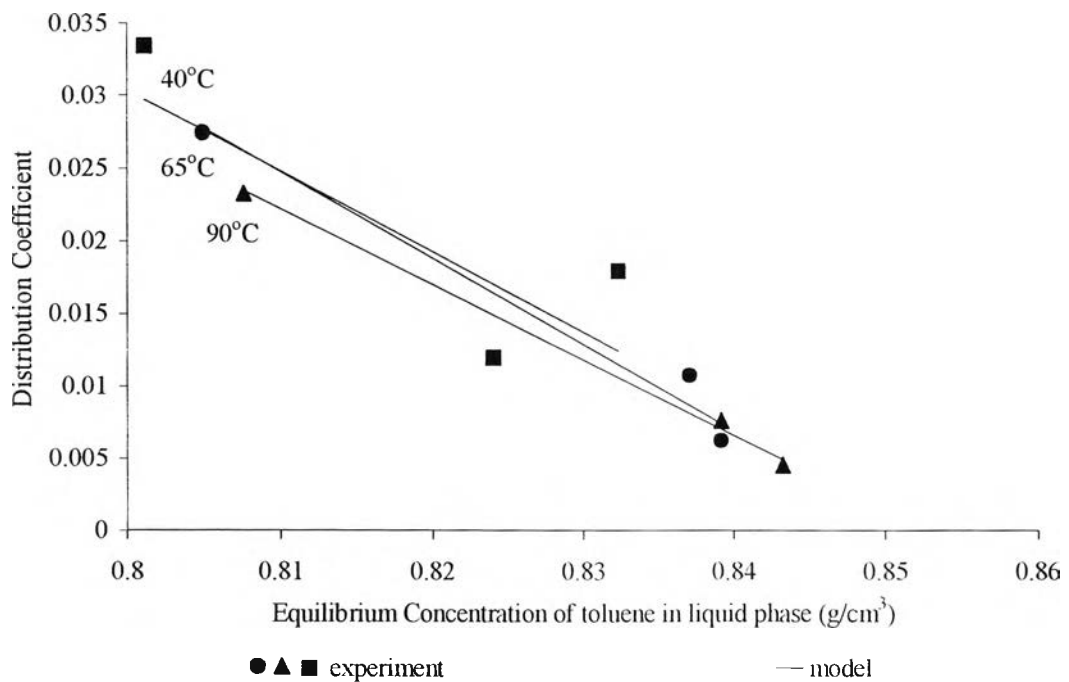

Figure 4.36 Comparison of experimental data and model prediction of toluene on the *KY* zeolite in *m*-xylene /toluene at 40, 65 and 90°C.
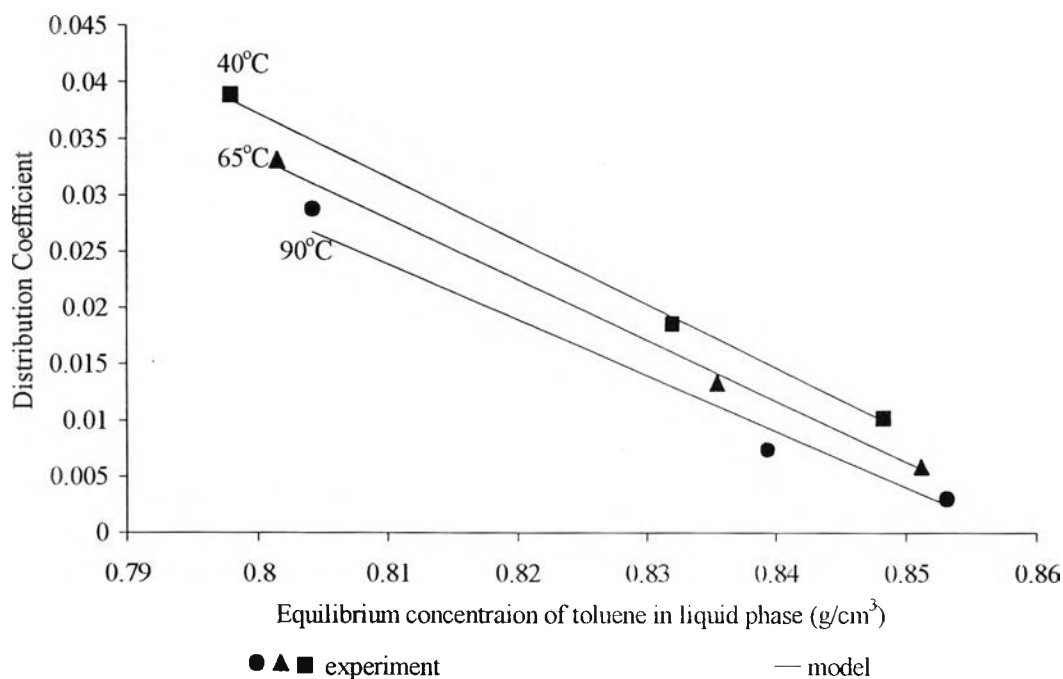
Figure 4.37 Comparison of experimental data and model prediction of toluene on the *KY* zeolite in ethylbenzene/toluene at 40, 65 and 90°C.
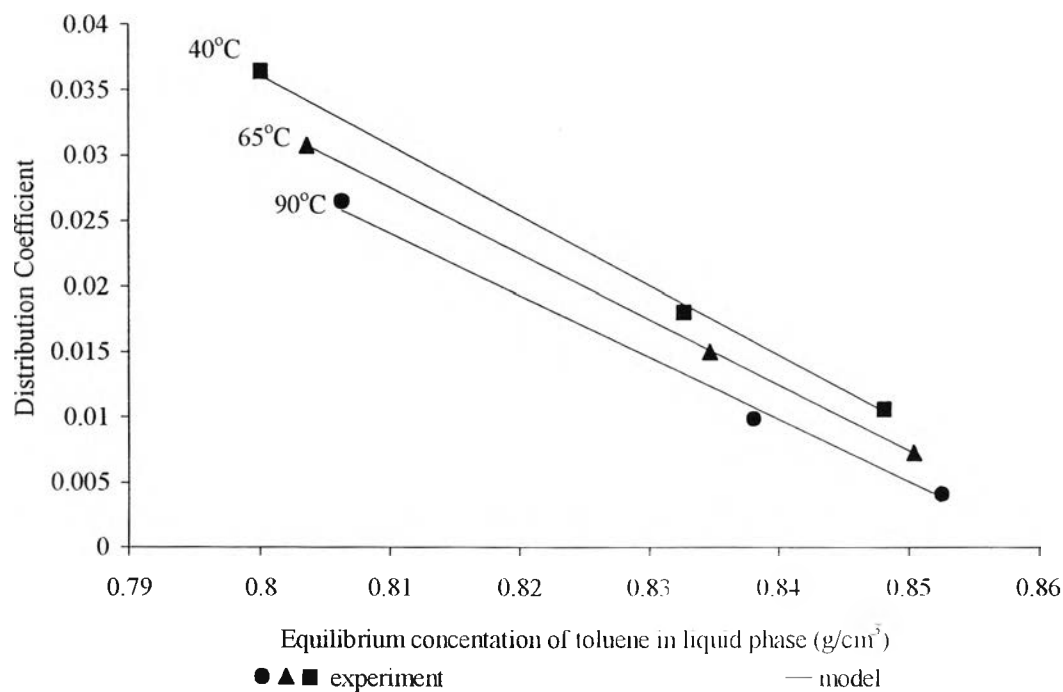

Figure 4.38 Comparison of experimental data and model prediction of toluene on the *KY* zeolite in *o*-xylene/toluene at 40, 65 and 90°C.